Systematic analysis of the *Myxococcus xanthus* developmental gene regulatory network supports posttranslational regulation of FruA by C-signaling

Running title: C-signaling regulates FruA posttranslationally

Shreya Saha[1], Pintu Patra[2], Oleg Igoshin[2], Lee Kroos[1*]

[1]Department of Biochemistry and Molecular Biology, Michigan State University, East Lansing, MI 48824, USA.

[2]Department of Bioengineering, Rice University, Houston, TX 77030, USA.

For correspondence. [*]E-mail kroos@msu.edu; Tel. (+1) 517 355 9726; Fax (+1) 517 353 9334.

Keywords: gene regulatory networks, signal transduction, transcription factors, developmental genes, bacterial spores, *Myxococcus xanthus*

Acknowledgements

We thank Monique Floer for advice about high-throughput qPCR and for use of the LightCycler® 480 System. We thank Montserrat Elias-Arnanz and Penelope Higgs for sharing strains. This work was supported by the National Science Foundation (award MCB-1411272) and by salary support for L.K. from Michigan State University AgBioResearch.

22 **Systematic analysis of the *Myxococcus xanthus* developmental gene regulatory network supports**

23 **posttranslational regulation of FruA by C-signaling**

24

25 **Summary**

26 Upon starvation *Myxococcus xanthus* undergoes multicellular development. Rod-shaped cells move

27 into mounds in which some cells differentiate into spores. Cells begin committing to sporulation at 24-

28 30 h poststarvation, but the mechanisms governing commitment are unknown. FruA and MrpC are

29 transcription factors that are necessary for commitment. They bind cooperatively to promoter regions

30 and activate developmental gene transcription, including that of the *dev* operon. Leading up to and

31 during the commitment period, *dev* mRNA increased in wild type, but not in a mutant defective in C-

32 signaling, a short-range signaling interaction between cells that is also necessary for commitment. The

33 C-signaling mutant exhibited ~20-fold less *dev* mRNA than wild type at 30 h poststarvation, despite a

34 similar level of MrpC and only twofold less FruA. Boosting the FruA level twofold in the C-signaling

35 mutant had little effect on the *dev* mRNA level, and *dev* mRNA was not less stable in the C-signaling

36 mutant. Neither did high cooperativity of MrpC and FruA binding upstream of the *dev* promoter

37 explain the data. Rather, our systematic experimental and computational analyses support a model in

38 which C-signaling activates FruA at least ninefold posttranslationally in order to commit a cell to spore

39 formation.

40

41 Keywords: gene regulatory networks, signal transduction, transcription factors, developmental genes,

42 bacterial spores, *Myxococcus xanthus*

43

44 **Introduction**

45 Differentiated cell types are a hallmark of multicellular organisms. Understanding how pluripotent
46 cells become restricted to particular cell fates is a fascinating question and a fundamental challenge in
47 biology. In general, the answer involves a complex interplay between signals and gene regulation. This
48 is true both during development of multicellular eukaryotes (Davidson & Levine, 2008, Frum & Ralston,
49 2015, Drapek *et al.*, 2017) and during transitions in microbial communities that lead to different cell
50 types (van Gestel *et al.*, 2015, Norman *et al.*, 2015, Bush *et al.*, 2015, Kroos, 2017). Bacterial cells in
51 microbial communities adopt different fates as gene regulatory networks (GRNs) respond to a variety
52 of signals, including some generated by other cells. Moreover, we now understand that microbial
53 communities or microbiomes profoundly impact eukaryotic organisms, and vice versa (Barratt *et al.*,
54 2017, Jansson & Hofmockel, 2018). Yet the daunting complexity of microbiomes and multicellular
55 eukaryotes impedes efforts to fully understand their interactions in molecular detail. By studying
56 simpler model systems, paradigms can be discovered that can guide investigations of more complex
57 interactions.

58 A relatively simple model system is provided by the bacterium *Myxococcus xanthus*, which
59 undergoes starvation-induced multicellular development (Yang & Higgs, 2014). In response to
60 starvation, cells generate intracellular and extracellular signals that regulate gene expression (Bretl &
61 Kirby, 2016, Kroos, 2017). The rod-shaped cells alter their movements so that thousands form a
62 mound. Within a mound, cells differentiate into ovoid spores that resist stress and remain dormant
63 until nutrients reappear. The spore-filled mound is called a fruiting body. Other cells adopt a different
64 fate and remain outside the fruiting body as peripheral rods (O'Connor & Zusman, 1991). A large
65 proportion of the cells lyse during the developmental process (Lee *et al.*, 2012). What determines

66 whether a given cell in the population forms a spore, remains as a peripheral rod, or undergoes lysis?
67 *M. xanthus* provides an attractive model system to discover how signaling between cells affects a GRN
68 and determines cell fate. Here, we focus on a circuit that regulates commitment to sporulation.
69 In a recent study, cells committed to spore formation primarily between 24 and 30 h poststarvation
70 (PS), because addition of nutrients to the starving population prior to 24 h PS blocked subsequent
71 sporulation, addition at 24 h PS allowed a few spores to form subsequently, and addition at 30 h PS
72 allowed about tenfold more spores to form (Rajagopalan & Kroos, 2014). At the molecular level,
73 addition of nutrients before or during the commitment period caused rapid proteolysis of MrpC
74 (Rajagopalan & Kroos, 2014), a transcription factor required for fruiting body formation (Sun & Shi,
75 2001b, Sun & Shi, 2001a).
76 MrpC appears to directly regulate more than one hundred genes involved in development
77 (Robinson *et al.*, 2014), and one well-characterized MrpC target gene, *fruA* (Ueki & Inouye, 2003),
78 codes for another transcription factor required for fruiting body formation (Ogawa *et al.*, 1996). FruA
79 and MrpC bind cooperatively to the promoter regions of many genes, and appear to activate
80 transcription (Campbell *et al.*, 2015, Lee *et al.*, 2011, Mittal & Kroos, 2009a, Mittal & Kroos, 2009b,
81 Robinson et al., 2014, Son *et al.*, 2011). In particular, transcription of the *dev* operon appears to be
82 activated by cooperative binding of the two transcription factors at two sites located upstream of the
83 promoter (Campbell et al., 2015). Because mutations in three genes of the *dev* operon (*devTRS*)
84 strongly impair sporulation (Boysen *et al.*, 2002, Thony-Meyer & Kaiser, 1993, Viswanathan *et al.*,
85 2007a), the feed-forward loop involving MrpC and FruA regulation of the *dev* operon is an attractive
86 molecular mechanism to control spore formation (Fig. 1). Recent work revealed that products of the
87 *dev* operon act as a timer for sporulation (Rajagopalan & Kroos, 2017). DevTRS negatively autoregulate

88 expression of DevI, which inhibits sporulation if overproduced, and delays sporulation by about 6 h
89 when produced normally (Rajagopalan & Kroos, 2017, Rajagopalan *et al.*, 2015) (Fig. 1).
90 Expression of the *dev* operon and many other developmental genes depends on C-signaling (Kroos
91 & Kaiser, 1987), which has been proposed to activate FruA (Ellehauge *et al.*, 1998) and/or MrpC (Mittal
92 & Kroos, 2009a) (Fig. 1), although the mechanism of C-signal transduction remains a mystery. Null
93 mutations in the *csgA* gene block C-signaling and sporulation, but the mutants can be rescued by co-
94 development with *csgA*$^+$ cells which supply the C-signal (Shimkets *et al.*, 1983). C-signaling appears to
95 be a short-range signaling interaction that requires cells to move into alignment (Kim & Kaiser, 1990c,
96 Kim & Kaiser, 1990b, Kroos *et al.*, 1988), as they do during mound formation (Sager & Kaiser, 1993).
97 Two theories about the identity of the C-signal have emerged. One theory states that the C-signal is a
98 17-kDa fragment of CsgA produced by the specific proteolytic activity of PopC at the cell surface (Kim &
99 Kaiser, 1990a, Lobedanz & Sogaard-Andersen, 2003, Rolbetzki *et al.*, 2008). The other theory is that
100 diacylglycerols released from the inner membrane by cardiolipin phospholipase activity of intact CsgA
101 are the C-signal (Boynton & Shimkets, 2015). However, in neither case has the signal receptor been
102 identified, so our understanding of C-signaling is incomplete. Likewise, how C-signaling impacts
103 recipient cells is unknown.
104 One way that C-signaling has been proposed to affect recipient cells is to stimulate
105 autophosphorylation of a histidine protein kinase, which would then transfer the phosphate to FruA
106 (Ellehauge et al., 1998). This model was attractive because FruA is similar to response regulators of
107 two-component signal transduction systems (Ellehauge et al., 1998, Ogawa et al., 1996). Typically, a
108 response regulator is phosphorylated by a histidine protein kinase in response to a signal, thus
109 activating the response regulator to perform a function (Stock *et al.*, 2000). The effects of substitutions

110 at the predicted site of phosphorylation in FruA supported the model that FruA is activated by
111 phosphorylation on D59 (Ellehauge et al., 1998). However, a histidine protein kinase capable of
112 phosphorylating FruA has not been identified. Also, several observations suggest that FruA may not be
113 phosphorylated. Most notably, D59 of FruA is present in an atypical receiver domain that lacks a
114 conserved metal-binding residue normally required for phosphorylation to occur, and treatment of
115 FruA with small-molecule phosphodonors did not increase its DNA-binding activity (Mittal & Kroos,
116 2009a). The receiver domain of FruA was shown to be necessary for cooperative binding with MrpC to
117 DNA, so it was proposed that C-signaling may affect activity of MrpC and/or FruA (Mittal & Kroos,
118 2009a) (Fig. 1).

119 The regulation of MrpC has been reported to be complex, involving autoregulation,
120 phosphorylation, proteolytic processing, binding to a toxin protein, and stability (Sun & Shi, 2001b,
121 Nariya & Inouye, 2005, Nariya & Inouye, 2006, Nariya & Inouye, 2008, Schramm *et al.*, 2012,
122 Rajagopalan & Kroos, 2014, McLaughlin *et al.*, 2018). Also, since MrpC is similar to CRP family
123 transcription factors that bind cyclic nucleotides (Sun & Shi, 2001b), MrpC activity could be modulated
124 by nucleotide binding, so there are many ways in which C-signaling could affect MrpC activity (Mittal &
125 Kroos, 2009a).

126 Here, using synergistic experimental and computational approaches, we investigate the impact of
127 C-signaling on a circuit that regulates commitment to sporulation by focusing on the feed-forward loop
128 involving MrpC and FruA control of *dev* operon transcription (Fig. 1). We describe methods to
129 systematically and quantitatively study the developmental process. Using these methods we measure
130 the levels of GRN components in wild type and in mutants (e.g., a *csgA* mutant unable to produce C-
131 signal) during the period leading up to and including commitment to spore formation. We then

132 formulate a mathematical model for the steady-state concentration of *dev* mRNA and use the model to
133 computationally predict the magnitude of potential regulatory effects of C-signaling that would be
134 required to explain our data. By testing the predictions, some potential regulatory mechanisms are
135 ruled out and at least ninefold activation of FruA by C-signaling is supported.
136

137 **Results**

138 **M. xanthus *development can be studied systematically***

139 We first established quantitative assays to analyze cellular and molecular changes during *M. xanthus*
140 development. To facilitate collection of sufficient cell numbers for counting, as well as for RNA and
141 protein measurements, development was induced by starvation under submerged culture conditions.
142 Cells adhere to the bottom of a plastic well or dish, and develop under a layer of buffer. Prior to cell
143 harvest, photos were taken to document phenotypic differences between strains. As expected, wild-
144 type strain DK1622 formed mounds by 18 h poststarvation (PS) and the mounds matured into
145 compact, darkened fruiting bodies at 36 to 48 h PS (Fig. 2). In contrast, *csgA* and *fruA* null mutants
146 failed to progress beyond forming loose aggregates. A *devI* null mutant was similar to wild type (WT),
147 whereas a *devS* null mutant formed mounds slowly and they failed to darken. Developing populations
148 were harvested at the times indicated in Figure 2 to measure cellular and molecular changes.

149 To quantify changes at the cellular level, we counted the total number of cells (after fixation and
150 dispersal, so that rod-shaped cells, spores, and cells in transition between the two were counted) and
151 the number of sonication-resistant spores in the developing populations. We also counted the number
152 of rod-shaped cells at the time when development was initiated by starvation (T_0). By subtracting the
153 number of sonication-resistant spores from the total cell number, we determined the number of

154 sonication-sensitive cells. About 30% of the wild-type cells present at T_0 remained as sonication-
155 sensitive cells at 18 h PS (Fig. S1A), consistent with the suggestion that the majority of cells lyse early
156 during development under submerged culture conditions, which was based on the decrease in the
157 total protein concentration of developing cultures (Rajagopalan & Kroos, 2014). The number of
158 sonication-sensitive cells continued to decline after 18 h PS, reaching ~4% of the T_0 number by 48 h PS
159 (Fig. S1A). Spores were first observed at 27 h PS and the number rose to ~1% of the T_0 number by 48 h
160 PS (Fig. S1B). The *devI* mutant was similar to WT, except spores were first observed 6 h earlier at 21 h
161 PS, as reported recently (Rajagopalan & Kroos, 2017). The *csgA*, *fruA*, and *devS* mutants failed to make
162 a detectable number of spores (at a detection limit of 0.04% of the T_0 number) and appeared to be
163 slightly delayed relative to WT and the *devI* mutant in terms of the declining number of sonication-
164 sensitive cells (Fig. S1 and Table S1). We conclude that at the cellular level during the time between 18
165 and 30 h PS (when we measured RNA and protein levels as described below), the developing
166 populations decline from 36 ± 4% to 16 ± 6% of the initial rod number and only 0.5 ± 0.2% (WT, *devI*) or
167 <0.04% (*csgA*, *fruA*, *devS*) of the cells form sonication-resistant spores (from which the RNAs and
168 proteins we measured would not be recovered based on control experiments). We stopped collecting
169 samples at 30 PS because thereafter the number of sonication-sensitive cells continues to decline and
170 the spore number continues to rise, making RNA and protein more difficult to recover quantitatively,
171 yet many cells are committed at 30 h PS to make spores by 36 h PS even if nutrients are added
172 (Rajagopalan & Kroos, 2014). Hence, we focused on changes at the molecular level between 18 and 30
173 h PS, the period leading up to and including the time that many cells commit to spore formation. We
174 acknowledge that the populations also contain cells destined to lyse or become peripheral rods, so the
175 magnitude of molecular changes required to commit a cell to the spore fate may be greater than

176 revealed by our population measurements. However, methods of rapidly separating all three cell types
177 from populations or of analyzing molecular changes in individual cells have not yet been reported.
178 To measure RNA levels of a large number of samples, we adapted methods described previously
179 (Rajagopalan & Kroos, 2014) to a higher-throughput robotic platform for RT-qPCR analysis.
180 Reproducibility of the analysis was tested among biological replicates and two types of technical
181 replicates as illustrated in Figure S2A, for each RNA to be measured, at 24 h PS, the midpoint of our
182 focal period. No normalization was done in this experiment. Each transcript number was derived from
183 a standard curve of genomic DNA subjected to qPCR. For each RNA, we found that the average
184 transcript number and the standard deviation for three cDNA technical replicates from a single RNA
185 sample, three RNA technical replicates from a single biological replicate, and three biological
186 replicates, was not significantly different (single factor ANOVA, $\alpha = 0.05$) (Fig. S2B-S2E). These results
187 suggest that biological variation in RNA levels at 24 h PS is comparable to technical variation in
188 preparing RNA and cDNA. In subsequent experiments, we measured RNA for at least three biological
189 replicates and we did not perform RNA or cDNA technical replicates. We also note the high abundance
190 of the *mrpC* transcript (~10%) relative to 16S rRNA, and the lower relative abundance of the *fruA* (~1%)
191 and *dev* (~0.1%) transcripts.
192 We have typically used 16S rRNA as an internal standard for RT-qPCR analysis during *M. xanthus*
193 development (Rajagopalan & Kroos, 2014). The high abundance of *mrpC* transcript relative to 16S
194 rRNA at 24 h PS (Fig. S2B and S2E) raised the possibility that rRNA decreases relative to total RNA at 18
195 to 30 h PS. To test this possibility, we measured the 16S rRNA level per μg of total RNA from 18 to 30 h
196 PS. Figure S3A shows that the level does not change significantly (single factor ANOVA, $\alpha = 0.05$),
197 validating 16S rRNA as an internal standard for subsequent experiments. We also found that the total

198 RNA yield per cell does not change significantly from 18 to 30 h PS (single factor ANOVA, $\alpha = 0.05$) (Fig.
199 S3B), consistent with the finding that the 16S rRNA level does not change significantly, since the
200 majority of total RNA is rRNA.

201 To measure protein levels, a portion of each well-mixed developing population was immediately
202 added to sample buffer, boiled, and frozen for subsequent semi-quantitative immunoblot analysis
203 (Rajagopalan & Kroos, 2017). The rest of the population was used for cell counting and RNA analysis as
204 described above and in the Experimental Procedures.

205

206 ***Levels of MrpC and FruA fail to account for the low level of* dev *mRNA in a* csgA *mutant***

207 By systematically quantifying protein and mRNA levels during the period leading up to and including
208 the time that cells commit to spore formation, we investigated whether the GRN shown in Figure 1
209 could account for observed changes over time in WT and in mutants. In particular, we were interested
210 in whether changes in the levels of MrpC and/or FruA proteins could account for the observed changes
211 in the level of *dev* mRNA, since MrpC and FruA bind cooperatively to the *dev* promoter region and
212 activate transcription (Campbell et al., 2015). In WT, we found that the MrpC level decreased about
213 1.5-fold on average from 18 to 30 h PS (Fig. 3A) and the FruA level rose about 1.5-fold on average (Fig.
214 3B), whereas the *dev* mRNA level rose about threefold on average (Fig. 4A). In each case, the fold-
215 change was small and the variation between biological replicates was large, so the result of a single
216 factor ANOVA ($\alpha = 0.05$) for each time course did not support a significant difference. We reasoned
217 that cooperative binding of MrpC and FruA could easily account for the threefold rise on average in *dev*
218 mRNA. We also measured the levels of *mrpC* and *fruA* mRNA. The *mrpC* mRNA level changed very
219 little on average (Fig. 4B), but the *fruA* mRNA level decreased about twofold on average after 18 h PS

220 (Fig. 4C), in contrast to the 1.5-fold rise on average in the FruA protein level (Fig. 3B), suggesting weak
221 positive posttranscriptional regulation of the FruA level during the period of commitment to spore
222 formation.

223 To investigate how C-signaling affects the GRN shown in Figure 1, we measured protein and mRNA
224 levels in the *csgA* null mutant. In agreement with earlier studies suggesting that C-signaling activates
225 FruA (Ellehauge et al., 1998) and/or MrpC (Mittal & Kroos, 2009a), we found very little *dev* mRNA in
226 the *csgA* mutant (Fig. 4A). Notably, the large decrease in the level of *dev* mRNA in the *csgA* mutant
227 compared with WT could not be accounted for by a large decrease in the level of MrpC or FruA. The
228 MrpC level was elevated about 1.5-fold on average in the *csgA* mutant relative to WT at most time
229 points (Fig. 3A), but the differences were not statistically significant ($p > 0.05$ in Student's two-tailed *t*-
230 tests comparing mutant to WT at each time point). The FruA level was diminished in the *csgA* mutant
231 relative to WT, but only about twofold on average (Fig. 3B). The differences in the FruA level were
232 statistically significant ($p < 0.05$ in Student's two-tailed *t*-tests) at each time point except 21 h PS ($p =$
233 0.12), but alone the twofold lower levels of FruA in the *csgA* mutant fail to account for the very low
234 levels of *dev* mRNA.

235 The *mrpC* and *fruA* mRNA levels were diminished about twofold and 1.5-fold on average,
236 respectively, in the *csgA* mutant relative to WT (Fig. 4B and 4C), but at nearly all time points the
237 differences were not statistically significant ($p > 0.05$ in Student's two-tailed *t*-tests, except $p = 0.03$ at
238 27 h for *mrpC* mRNA). The small differences in the level of *fruA* mRNA in the *csgA* mutant relative to
239 WT are especially noteworthy, since they imply that C-signaling has little or no effect on MrpC activity.
240 The results of our *fruA* mRNA measurements agree with published reports using *fruA-lacZ* fusions
241 (Ellehauge et al., 1998, Srinivasan & Kroos, 2004). Furthermore, we found that *fruA* mRNA stability is

242 similar in the *csgA* mutant and in WT at 30 h PS (Fig. S4), indicating that the similar steady-state *fruA*
243 mRNA level we observed (Fig. 4C) reflects a similar rate of synthesis, rather than altered synthesis
244 compensated by altered stability. We conclude that C-signaling does not affect MrpC activity.
245 Therefore, the low level of *dev* mRNA in a *csgA* mutant (Fig. 4A) could be due to failure to activate FruA
246 or to *dev*-specific regulatory mechanisms.

247 To begin to characterize potential *dev*-specific regulatory mechanisms during the period leading up
248 to and including commitment to sporulation, we measured protein and mRNA levels in the *devS* and
249 *devI* null mutants. The MrpC and FruA levels were similar to WT (Fig. 3). The *dev* mRNA level ranged
250 from 20-fold higher in the *devS* mutant than in WT at 18 h PS, to 10-fold higher at 30 h PS (Fig. 4A),
251 consistent with negative autoregulation by DevS (and DevT and DevR) reported previously
252 (Rajagopalan & Kroos, 2017, Rajagopalan et al., 2015). Unexpectedly, the *dev* mRNA level in the *devI*
253 mutant was about threefold lower than in WT at 30 h PS (Fig. 4A), suggesting that DevI feeds back
254 positively on accumulation of *dev* mRNA, although the difference was not quite statistically significant
255 at the 95% confidence level ($p = 0.06$ in Student's two-tailed *t*-test). Other differences were that the
256 *fruA* mRNA levels in the *devI* and *devS* mutants were about twofold lower than in WT at 27 and 30 h PS
257 (Fig. 4C), and these were statistically significant ($p < 0.05$ in Student's two-tailed *t*-tests comparing
258 mutant to WT at each time point). Since the FruA levels in these mutants were similar to those in WT
259 (Fig. 3B), positive posttranscriptional regulation of FruA appeared to occur in the mutants, as well as in
260 WT.

261 We also measured the *dev* mRNA level in a *ladA* null mutant, because LadA was reported to be a
262 strong positive regulator of *dev* expression based on analysis of transcriptional *lacZ* fusions
263 (Viswanathan *et al.*, 2007b). Although the *dev* mRNA was on average twofold lower in the *ladA* mutant

264 than in WT at 18 h PS and the difference was statistically significant ($p < 0.05$ in Student's two-tailed *t*-
265 tests), significant differences were not observed at 24 or 30 h (Fig. S5A). These results show that LadA
266 does not control the *dev* transcript level during the period (24 to 30 h PS) when cells commit to spore
267 formation under our conditions. Differences in the methods of measuring expression and/or the
268 developmental conditions may account for the different conclusion reached here about the effect of
269 LadA on *dev* expression, as compared with the previous study (Viswanathan et al., 2007b). We note
270 that, as in the previous study, the *ladA* mutant was delayed for mound formation and darkening (Fig.
271 S6A). Formation of sonication-resistant spores was also delayed (Fig. S6B).
272 To complete our characterization of the GRN shown in Figure 1, we also measured protein and
273 mRNA levels in the *fruA* and *mrpC* null mutants. We did not collect samples of the *mrpC* mutant at as
274 many time points since we expected little or no expression of GRN components. As expected, neither
275 MrpC nor FruA were detected in the *mrpC* mutant (Fig. S7). In the *fruA* mutant, the MrpC level was
276 similar to WT and, as expected, FruA was not detected (Fig. 3). Also as expected, in the *fruA* mutant
277 the *fruA* mRNA was not detected, the *dev* mRNA level was very low, and the *mrpC* mRNA level was
278 similar to WT (Fig. 4). Since the *mrpC* mutant had an in-frame deletion of codons 74 to 229 (Sun & Shi,
279 2001b), we were able to design primers for RT-qPCR analysis that should detect the shorter *mrpC*
280 transcript. Surprisingly, the *mrpC* mutant exhibited an elevated level of *mrpC* transcript compared with
281 WT at 18 and 24 h PS (Fig. S8A). The result was surprising since expression of an *mrpC-lacZ* fusion had
282 been reported to be abolished in the *mrpC* mutant, which had led to the conclusion that MrpC
283 positively autoregulates (Sun & Shi, 2001b). We considered the possibility that the shorter transcript in
284 the *mrpC* mutant is more stable than the WT transcript, but the transcript half-lives after addition of
285 rifampicin did not differ significantly (Fig. S9). We conclude that MrpC negatively regulates the *mrpC*

286 transcript level. While this work was in progress, McLaughlin *et al*. reached the same conclusion
287 (McLaughlin et al., 2018). In all other respects, the *mrpC* mutant yielded expected results. The *fruA*
288 and *dev* transcripts were very low (Fig. S8B and S8C), consistent with the expectations that MrpC is
289 required to activate *fruA* transcription (Ueki & Inouye, 2003) and that MrpC and FruA are required to
290 activate *dev* transcription (Campbell et al., 2015, Ellehauge et al., 1998, Viswanathan et al., 2007b).
291 Also, the *mrpC* mutant failed to progress beyond forming loose aggregates (Fig. S10), appeared to be
292 slightly delayed relative to WT in terms of the declining number of sonication-sensitive cells (Fig. S11A),
293 and failed to make a detectable number of spores (at a detection limit of 0.04% of the T_0 number) (Fig.
294 S11B).

295 Taken together, our systematic, quantitative measurements of components of the GRN shown in
296 Figure 1 imply that failure to activate FruA and/or *dev*-specific regulatory mechanisms may account for
297 the low level of *dev* mRNA in a *csgA* mutant. Given the complex feedback architecture of *dev*
298 regulation (i.e., strong negative feedback by DevTRS and weak positive feedback by DevI at 30 h PS),
299 delineating the effects of C-signaling on the *dev* transcript level requires a mathematical modeling
300 approach.

301

302 ***Mathematical modeling suggests several mechanisms that could explain the low level of dev mRNA***
303 ***in the* csgA *mutant***

304 The observed small differences in the levels of MrpC and FruA in the *csgA* mutant relative to WT do not
305 account for the very low level of *dev* mRNA in the *csgA* mutant. To evaluate plausible mechanisms that
306 may explain these experimental findings, we quantitatively analyzed transcriptional regulation of *dev*
307 by formulating a mathematical model that expresses the *dev* mRNA concentration as a function of the

308 regulators MrpC, FruA, DevI, and DevS. MrpC and FruA bind cooperatively to the *dev* promoter region

309 and activate transcription (Campbell et al., 2015). Our results suggest that DevI is a weak positive

310 regulator and DevS is a strong negative regulator of *dev* transcription by 30 h PS (Fig. 4A).

311 Incorporating these effects into a transcriptional regulation model, we express the concentration of

312 *dev* mRNA as a product of three regulation functions ($\Pi_{\mathrm{FM}}, \Pi_{\mathrm{I}}, \Pi_{\mathrm{S}}$) divided by the transcript

313 degradation rate δ_{dev} (see Experimental Procedures for detailed explanation):

314 $$[\mathrm{mRNA}_{dev}] = \frac{1}{\delta_{dev}} \underbrace{\left(\alpha_{\mathrm{FM}} \frac{\left(\frac{[\mathrm{FruA}][\mathrm{MrpC}]}{\mathrm{K_{FM}}}\right)^{a}}{1+\left(\frac{[\mathrm{FruA}][\mathrm{MrpC}]}{\mathrm{K_{FM}}}\right)^{a}} \right)}_{\Pi_{\mathrm{FM}}} \underbrace{\left(1+\alpha_{\mathrm{I}} \frac{\left(\frac{[\mathrm{DevI}]}{\mathrm{K_I}}\right)^{b}}{1+\left(\frac{[\mathrm{DevI}]}{\mathrm{K_I}}\right)^{b}} \right)}_{\Pi_{\mathrm{I}}} \underbrace{\left(\frac{1}{1+\left(\frac{[\mathrm{DevS}]}{\mathrm{K_S}}\right)^{c}} \right)}_{\Pi_{\mathrm{S}}}$$

315 Here, we use a quasi-steady state approximation for the mRNA levels by taking advantage of the fact

316 that mRNA decay (with half-lives typically in minutes) is much faster than our experimental

317 measurement times (in hours). This allows us to assume a rapid equilibrium between the rate of *dev*

318 transcription and the decay of its mRNA, which leads to the above equation, in which

319 $\alpha_{\mathrm{FM}}, \alpha_{\mathrm{I}}, \delta_{\mathrm{dev}}, \mathrm{a}, \mathrm{b}, \mathrm{c}, \mathrm{K_{FM}}, \mathrm{K_I}$ and $\mathrm{K_S}$ are parameters characterizing promoter regulation. We assume

320 that these biochemical parameters are not a function of the genetic background and, therefore, in the

321 strains in which *dev* mRNA was measured (e.g., the *csgA* mutant), the concentration of *dev* mRNA is

322 determined by the concentrations of proteins (indicated by square brackets in the equation), more

323 specifically the concentrations of their transcriptionally active forms (in case there is a

324 posttranslational regulation). To estimate how the different regulation parameters (such as

325 transcription rate, degradation rate, cooperativity constant, etc.) affect the *dev* mRNA level, we first

326 constrain the model parameters by the experimental result shown in Figure 3B, $[\mathrm{FruA}]_{\mathrm{WT}}/$

327 $[\mathrm{FruA}]_{csgA} \cong 2$, and search for parameters that can result in the observed 22-fold difference

328 in $[\mathrm{mRNA}_{dev}]$ in WT relative to the *csgA* mutant at 30 h PS (Fig. 4A).

329 To estimate the contribution of autoregulation by Dev proteins to their own transcription (i.e., the

330 terms $\Pi_{\mathrm{I}}, \Pi_{\mathrm{S}}$) in WT and the *csgA* mutant, we employ the data from the *devI* and *devS* mutants (Fig.

331 4A). Specifically, we take the ratio of the *dev* mRNA level in WT to that in *devI* and *devS* mutants to

332 estimate the feedback regulation from DevI and DevS, respectively (see Experimental Procedures for

333 details). We find the contribution from DevI and DevS feedback regulation in WT to be $\Pi_{\mathrm{I,WT}} = 2.9$

334 and $\Pi_{\mathrm{S,WT}} = 0.091$, respectively. Using these values, we find the contribution from FruA and MrpC

335 regulation to be $\Pi_{\mathrm{FM,WT}}/\delta_{dev,\mathrm{WT}} = 11$. In the *csgA* mutant, since the *dev* mRNA level is very low, we

336 assume the DevI and DevS protein levels to be low. This gives the contribution of different regulation

337 functions as $\Pi_{\mathrm{I},csgA} \approx 1$, $\Pi_{\mathrm{S},csgA} \approx 1$, and $\Pi_{\mathrm{FM},csgA}/\delta_{dev,csgA} = 0.13$. In summary, this analysis reveals

338 that the twofold reduction of FruA protein observed in the *csgA* mutant (Fig. 3B) leads to a change

339 of $(\Pi_{\mathrm{FM,WT}}/\Pi_{\mathrm{FM},csgA})(\delta_{dev,csgA}/\delta_{dev,\mathrm{WT}}) \approx 84$-fold in the FruA- and MrpC-dependent transcript

340 regulation term. We reasoned that the observed 22-fold reduction in *dev* transcript in the *csgA* mutant

341 relative to WT at 30 h PS (Fig. 4A) could result from a reduction in the FruA- and MrpC-dependent

342 activation rate Π_{FM} and/or an increase in the transcript degradation rate δ_{dev}. In what follows we use

343 the mathematical model to predict the magnitude of these effects that would be necessary to explain

344 the observed 22-fold difference in $[\mathrm{mRNA}_{dev}]$.

345 - **Hypothesis 1:** Increase in *dev* transcript degradation rate in the *csgA* mutant

346 First, we estimate the difference in *dev* transcript degradation rate necessary to explain the observed

347 difference in transcript level between WT and the *csgA* mutant. For this, we make two assumptions.

348 First, we assume that MrpC and FruA bind to the *dev* promoter region with a Hill cooperativity

349 coefficient $a = 2$ (i.e., the maximum for a single cooperative binding site). Second, we assume that the
350 observed twofold difference in FruA protein level results in a twofold difference in transcriptionally
351 active FruA. Under these assumptions, we vary the remaining unknown parameters to compute the
352 required fold difference in transcript degradation rate for different values of promoter saturation. Our
353 results plotted in Figure 5A show that at least a 20-fold difference in transcript degradation rate is
354 required to explain the transcript data. This experimentally testable prediction will be assessed in a
355 subsequent section. If the results are inconsistent with this prediction, we must conclude that at least
356 one of the two assumptions above is invalid, resulting in the following two alternative hypotheses: the
357 Hill coefficient of MrpC and FruA binding to the *dev* promoter region is much higher than $a = 2$ and/or
358 the amount of transcriptionally active FruA does not scale with the measured FruA protein level (e.g., if
359 *csgA*-dependent C-signaling is also involved in posttranslational activation of FruA).

360 - **Hypothesis 2:** High cooperativity of MrpC and FruA binding to the *dev* promoter region

361 Next, we test if a higher binding cooperativity can explain the difference in *dev* transcript level
362 between WT and the *csgA* mutant. We compute the required cooperativity coefficient by assuming
363 the degradation rate does not change between the two strains. Our results plotted in Figure 5B show
364 that the minimum cooperativity coefficient required to explain the experimental results is six for low
365 promoter saturation. In biologically realistic conditions, where promoter saturation is higher; the
366 required cooperativity is even higher. Such a large cooperativity can only be explained if there is more
367 than one site in the promoter region where MrpC and FruA bind with high cooperativity. We know
368 that the *dev* promoter region has at least two MrpC and FruA cooperative binding sites; one is proximal
369 upstream, whereas the other is distal upstream (Campbell et al., 2015). The distal upstream binding
370 site appeared to boost *dev* promoter activity after 24 h PS, based on β-galactosidase activity from a

371 *lacZ* reporter. Hence, in a subsequent section, we study the impact of a distal site deletion on different
372 transcripts (*mrpC, fruA, dev*) and proteins (MrpC, FruA) to test if presence of the distal site contributes
373 to higher cooperativity. If the results are not consistent with the model predictions, we must conclude
374 that the fold difference in active FruA exceeds that observed for the total concentration of each
375 protein (i.e., *csgA*-dependent C-signaling is involved in posttranslational activation of FruA).

376 - **Hypothesis 3:** Posttranslational regulation of FruA activity

377 To assess the difference in active FruA level required to explain the observed difference in *dev*
378 transcript level, in the absence of other effects, we fix the cooperativity coefficient at $a = 2$ and
379 assume the transcript degradation rate to be unchanged between WT and the *csgA* mutant. We then
380 use our model to compute the fold difference in active FruA required to achieve a 22-fold reduction in
381 *dev* transcript in the *csgA* mutant relative to WT. Our results plotted in Figure 5C show that at least a
382 ninefold reduction in active FruA is needed in the *csgA* mutant. The reduction in active FruA in the
383 *csgA* mutant would presumably be due to the absence of C-signal-dependent posttranslational
384 activation of FruA, not due to the twofold lower level of FruA protein we observed in the *csgA* mutant
385 relative to WT (Fig. 3B). The reduction in active FruA may be considerably greater than ninefold if the
386 *dev* promoter region approaches saturation (e.g., 20-fold at 80% saturation in Fig. 5C). Also,
387 mathematical modeling of our data at each time point from 18 to 30 h PS yields a similar result (Fig.
388 S12), suggesting that in WT, FruA has already been activated by C-signaling at least ninefold by 18 h PS,
389 and perhaps as much as 30-fold if the *dev* promoter region approaches saturation (righthand panel in
390 Fig. S12).

391

392 ***Stability of the* dev *transcript is unchanged in a* csgA *mutant***

393 To measure the *dev* transcript degradation rate in WT and the *csgA* mutant, we compared the *dev*
394 transcript levels after addition of rifampicin to block transcription at 30 h PS. The average half-life of
395 the *dev* transcript in three biological replicates was 11 ± 6 min in WT and 7 ± 1 min in the *csgA* mutant
396 (Fig. 6), which is not a statistically significant difference (p = 0.36 in a Student's two-tailed t-test). We
397 conclude that elevated turnover does not account for the low level of *dev* transcript in the *csgA*
398 mutant. These results allow us to rule out Hypothesis 1.
399
400 ***The distal upstream binding site for MrpC and FruA has little impact on the* dev *transcript level***
401 In a previous study, weak cooperative binding of MrpC and FruA to a site located between positions -
402 254 and -229 upstream of the *dev* promoter appeared to boost β-galactosidase activity from a *lacZ*
403 transcriptional fusion about twofold between 24 and 30 h PS, but deletion of the distal upstream site
404 did not impair spore formation (Campbell et al., 2015). These findings suggested that the distal site
405 has a modest impact on *dev* transcription that is inconsequential for sporulation. However, β-
406 galactosidase activity from *lacZ* fused to *dev* promoter segments with different amounts of upstream
407 DNA and integrated ectopically may not accurately reflect the contribution of the distal site to the *dev*
408 transcript level. Therefore, we measured the *dev* transcript level in a mutant lacking the distal site (i.e.,
409 DNA between positions -254 and -228 was deleted from the *M. xanthus* chromosome). The level of
410 *dev* transcript in the distal site mutant was similar to WT measured in the same experiment, in this
411 case increasing about twofold from 18 to 30 h PS (Fig. 7). Likewise, the levels of *mrpC* and *fruA*
412 transcripts (Fig. S8) and the corresponding proteins (Fig. S7) were similar in the distal site mutant as
413 compared with WT (p > 0.05 in Student's two-tailed t-tests comparing mutant to WT at each time
414 point, except p = 0.02 for *fruA* transcript levels at 18 h, p = 0.03 for MrpC protein levels at 30 h, and p =

415 0.03 for FruA protein levels at 18 h). The distal site mutant formed mounds by 18 h PS, which matured
416 into compact, darkened fruiting bodies at later times, similar to WT (Fig. S10), and the percentages of
417 sonication-sensitive cells and sonication-resistant spores observed for the distal site mutant were
418 similar to WT (Fig. S11). We conclude that the distal site has little or no impact on the developmental
419 process. In particular, the distal site does not contribute to high cooperativity of MrpC and FruA
420 binding to the *dev* promoter region that could explain the higher level of *dev* transcript in WT than in
421 the *csgA* mutant. These results allow us to rule out Hypothesis 2.
422
423 ***Boosting the FruA level in the* csgA *mutant has no effect on the* dev *transcript level***
424 Having ruled out the first two hypotheses, our modeling predicts that the only viable option to explain
425 the effect of the *csgA* null mutation on the *dev* transcript level is Hypothesis 3: at least a ninefold
426 reduction in active FruA is needed in the *csgA* mutant as compared with WT. Specifically, our model
427 showed that the low *dev* transcript level in the *csgA* mutant is not due to its twofold lower FruA level
428 (Fig. 3B), but rather due to a failure to activate FruA in the absence of C-signaling (Fig. 5C and S12). As
429 a result, the model predicts that in the *csgA* mutant most of the FruA remains inactive. To test this
430 prediction, we integrated *fruA* transcriptionally fused to a vanillate-inducible promoter ectopically in
431 the *csgA* mutant. Upon induction the *csgA* P_{van}-*fruA* strain accumulated a similar level of FruA as WT
432 (Fig. 8A), but the *dev* transcript level remained as low as in the *csgA* mutant (Fig. 8B). Hence, boosting
433 the FruA level in the *csgA* mutant had no effect on the *dev* transcript level, consistent with our
434 prediction and supporting the hypothesis that C-signaling activates FruA at least ninefold.
435 Additionally, we tested the previously proposed model that C-signal-dependent phosphorylation of
436 D59 activates FruA (Ellehauge et al., 1998). We created *fruA D59E*, an allele designed to produce FruA

437 D59E with a phosphomimetic substitution in its receiver domain. In some cases, such a substitution
438 causes a response regulator to be constitutively active (Domian *et al.*, 1997, Klose *et al.*, 1993, Lan &
439 Igo, 1998), including response regulators in the NarL/FixJ subfamily to which FruA belongs (Davlieva *et*
440 *al.*, 2015, Galperin, 2010, Ellehauge et al., 1998). Therefore, if FruA is normally activated by
441 phosphorylation of D59 in response to C-signaling, expression of *fruA D59E* may restore the *dev*
442 transcript level in the *csgA* mutant. We integrated *fruA D59E* transcriptionally fused to a vanillate-
443 inducible promoter ectopically in the *csgA* mutant. Upon induction the *csgA* P_{van}-*fruA D59E* strain
444 accumulated FruA D59E to a similar level as FruA accumulated by WT (Fig. 8A), but the *dev* transcript
445 level in the *csgA* P_{van}-*fruA D59E* strain remained as low as in the *csgA* mutant (Fig. 8B). These results
446 suggest that D59 phosphorylation may not be the mechanism by which C-signaling activates FruA.
447 The *fruA* transcript (Fig. S13A), *mrpC* transcript (Fig. S13B), and MrpC protein (Fig. S14) levels were
448 similar in the *csgA* P_{van}-*fruA* and *csgA* P_{van}-*fruA D59E* strains as in WT and the *csgA* mutant. Induction
449 of the *csgA* P_{van}-*fruA* and *csgA* P_{van}-*fruA D59E* strains did not rescue development, which failed to
450 progress beyond forming loose aggregates (Fig. S15), and the strains failed to make a detectable
451 number of spores by 48 h PS (Table S1). The induced *csgA* P_{van}-*fruA* strain appeared to be slightly
452 delayed relative to WT in terms of the declining number of sonication-sensitive cells, like the *csgA*
453 mutant, whereas the induced *csgA* P_{van}-*fruA D59E* appeared to be defective in attachment, resulting in
454 recovery of less sonication-sensitive cells at 18 h PS (Fig. S16).
455 As controls, P_{van}-*fruA* and P_{van}-*fruA D59E* were integrated ectopically in the *fruA* mutant. Upon
456 induction the *fruA* P_{van}-*fruA* strain formed mounds by 18 h PS and the mounds matured into compact,
457 darkened fruiting bodies at later times, similar to WT without or with vanillate added (Fig. S17). The
458 induced *fruA* P_{van}-*fruA D59E* strain formed mounds by 24 h PS, which matured into compact, darkened

459 fruiting bodies, similar to WT. Also, the induced *fruA* P_{van}-*fruA* and P_{van}-*fruA D59E* strains exhibited a
460 similar number of sonication-resistant spores as WT at 36 h PS (data not shown). These results show
461 that induction of the *fruA* P_{van}-*fruA* and *fruA* P_{van}-*fruA D59E* strains rescued development, presumably
462 because C-signaling activated the FruA and FruA D59E produced, respectively.

463 ***Other FruA-dependent transcripts are present at very low levels in the* csgA *mutant, even when FruA***
464 ***or FruA D59E is produced***

465 In addition to the *dev* operon, four other genes or operons appear to be activated by cooperative
466 binding of FruA and MrpC in their promoter region (Lee et al., 2011, Mittal & Kroos, 2009a, Mittal &
467 Kroos, 2009b, Son et al., 2011). These genes, designated *fmg* for "FruA- and Mrp-regulated gene", also
468 depend on C-signaling for expression, based on analysis of *lacZ* fusions (Kroos & Kaiser, 1987). We
469 measured the levels of *fmgA*, *fmgBC*, *fmgD*, and *fmgE* transcripts in the *csgA* mutant and the induced
470 *csgA* P_{van}-*fruA* and *csgA* P_{van}-*fruA D59E* strains during development. Like the *dev* transcript level (Fig.
471 8B), the *fmg* transcript levels were very low in the *csgA* mutant and in its derivatives induced to
472 produce FruA or FruA D59E (Fig. S18). These findings support the hypothesis that C-signaling activates
473 FruA and that it may do so by a mechanism other than D59 phosphorylation.

474 To investigate whether LadA regulates *fmg* genes, we measured *fmg* transcript levels in the *ladA*
475 null mutant. Like the *dev* transcript level (Fig. S5A), the *fmgA* and *fmgD* transcript levels were
476 significantly lower in the *ladA* mutant than in WT at 18 h PS ($p < 0.05$ in Student's two-tailed *t*-tests),
477 but not at 24 or 30 h (Fig. S5B and S5D). The *fmgBC* and *fmgE* transcript levels were significantly lower
478 in the *ladA* mutant at 18 and 24 h, and at all three times, respectively (Fig. S5C and S5E). Hence, LadA
479 does not control the *fmgA* and *fmgD* transcript levels during the period (24 to 30 h PS) when cells
480 commit to spore formation under our conditions, but LadA appears to positively regulate the *fmgBC*

481 transcript level twofold on average at 24 h and the *fmgE* transcript level about fivefold on average at
482 24 to 30 h.
483
484 **Discussion**
485 Our systematic, quantitative analysis of a key circuit in the GRN governing *M. xanthus* fruiting body
486 formation implicates posttranslational regulation of FruA by C-signaling as primarily responsible for *dev*
487 transcript accumulation during the period leading up to and including commitment to spore formation.
488 Mathematical modeling of the *dev* transcript level allowed us to predict the magnitude of potential
489 regulatory mechanisms. Experiments ruled out C-signal-dependent stabilization of *dev* mRNA or highly
490 cooperative binding of FruA and MrpC to two sites in the *dev* promoter region as the explanation for
491 the much higher *dev* transcript level in WT than in the *csgA* mutant. Although the FruA level was
492 twofold lower in the *csgA* mutant than in WT (Fig. 3B and 8A), boosting the FruA or FruA D59E level in
493 the *csgA* mutant had no effect on the *dev* transcript level (Fig. 8B) and did not rescue development
494 (Fig. S15). Taken together, our experimental and computational analyses provide evidence that C-
495 signaling activates FruA at least ninefold posttranslationally during *M. xanthus* development (Fig. 9),
496 and likely by a mechanism other than phosphorylation of D59. The activation of FruA may be
497 considerably greater than ninefold if the *dev* promoter region approaches saturation (Fig. 5C and S12).
498 Since efficient C-signaling requires cells to move into close proximity (Kim & Kaiser, 1990c, Kim &
499 Kaiser, 1990b, Kroos et al., 1988), we propose that activation of FruA by C-signaling acts as a
500 checkpoint for mound formation during the developmental process (Fig. 9).
501
502 ***Regulation of FruA by C-signaling***

503 If activation of FruA by C-signaling acts as a checkpoint for mound formation, then active FruA should
504 be present at 18 h PS since mound formation is well underway (Fig. 2). In agreement, mathematical
505 modeling of our data using the assumptions of hypothesis 3 at each time point from 18 to 30 h PS
506 yields a similar result (Fig. S12). This analysis implies that FruA has already been activated by C-
507 signaling at least ninefold by 18 h PS, if the assumptions of hypothesis 3 apply. The assumption that
508 the distal site does not contribute to high cooperativity of MrpC and FruA binding to the *dev* promoter
509 region applies since the *dev* transcript level did not differ significantly in the distal site mutant as
510 compared with WT at 18 or 24 h PS (Fig. 7). We did not measure *dev* transcript stability at 18 to 27 h
511 PS, but at 30 h PS there was no significant difference between WT and the *csgA* mutant (Fig. 6).
512 Therefore, C-signaling may have already activated FruA at least ninefold by 18 h PS, and perhaps as
513 much as 30-fold if the *dev* promoter region approaches saturation (90% saturation in the righthand
514 panel of Fig. S12). We note that during the period from 18 to 30 h PS, the *dev* transcript level rises, but
515 the rise is due to positive autoregulation by DevI (Fig. 4A). Hence, active FruA may not be the limiting
516 factor for *dev* transcription during this period (i.e., the *dev* promoter region may indeed approach
517 saturation binding of active FruA and MrpC). The proximal upstream site in the *dev* promoter region,
518 which is crucial for transcriptional activation, exhibits a higher affinity for cooperative binding of FruA
519 and MrpC than the distal upstream site (Campbell et al., 2015) or several other sites (Robinson et al.,
520 2014, Son et al., 2011), perhaps conferring on *dev* transcription a relatively low threshold for active
521 FruA.

522 The mechanism of FruA activation by C-signaling is unknown. Since FruA is similar to response
523 regulators of two-component signal transduction systems, phosphorylation by a histidine protein
524 kinase was initially proposed to control FruA activity (Ellehauge et al., 1998, Ogawa et al., 1996). While

525 this potential mechanism of posttranslational control cannot be ruled out, a kinase capable of
526 phosphorylating FruA has not been identified despite considerable effort. Moreover, the atypical
527 receiver domain of FruA and the inability of small-molecule phosphodonors to increase its DNA-binding
528 activity suggest that FruA may not be phosphorylated (Mittal & Kroos, 2009a). In further support of
529 this possibility, we found that expression of FruA D59E, designed to mimic phosphorylation of the
530 receiver domain, did not appear to constitutively activate the protein in the absence of C-signaling (Fig.
531 8 and S15). Neither did the D59E substitution render FruA unable to be activated, since expression of
532 FruA D59E rescued development of the *fruA* mutant (Fig. S17), consistent a previous study (Ellehauge
533 et al., 1998). Hence, FruA may be an atypical response regulator that is activated by C-signaling *via* a
534 mechanism other than phosphorylation.

535 Several atypical response regulators have been shown to be active without phosphorylation and a
536 few are regulated by ligand binding (Bourret, 2010, Desai *et al.*, 2016). For example, the atypical
537 receiver domain of *Streptomyces venezuelae* JadR1 is bound by jadomycin B, causing JadR1 to
538 dissociate from DNA, and the acylated antibiotic undecylprodigiosin of *Streptomyces coelicolor* may
539 use a similar mechanism to modulate DNA-binding activity of the atypical response regulator RedZ
540 (Wang *et al.*, 2009). Conceivably, FruA activity could likewise be regulated by binding of *M. xanthus*
541 diacylglycerols, which have been implicated in C-signaling (Boynton & Shimkets, 2015). Alternatively,
542 FruA could be regulated by a posttranslational modification other than phosphorylation or by binding
543 to another protein (i.e., sequestration).

544 In addition to regulating FruA activity posttranslationally, C-signaling appears to regulate the FruA
545 level posttranscriptionally. The FruA level was reproducibly twofold lower in the *csgA* mutant than in
546 WT (Fig. 3B and 8A), but the *fruA* transcript level was not significantly different (Fig. 4C and S11A).

547 These results suggest that positive posttranscriptional regulation of the FruA level requires C-signaling.
548 C-signaling may increase synthesis (i.e., increase *fruA* mRNA accumulation slightly and also increase
549 translation of *fruA* mRNA) and/or decrease turnover of FruA. We did not investigate this further
550 because the FruA deficit in the *csgA* mutant could be overcome with P_{van}-*fruA* or P_{van}-*fruA D59E*, yet
551 there was very little effect on the *dev* transcript level (Fig. 8). This demonstrates that the activity of
552 FruA, rather than its level, primarily controls the level of *dev* transcript.
553
554 ***Regulation by Dev proteins***
555 DevI inhibits sporulation if overexpressed, as in the *devS* mutant (Rajagopalan et al., 2015) (Fig. 2 and
556 S1). Deletion of *devI* or the entire *dev* operon allows spores to begin forming about 6 h earlier than
557 normal, but does not increase the final number of spores (Rajagopalan & Kroos, 2017) (Fig. S1). The
558 level of MrpC was about twofold higher on average in the *devI* mutant than in WT at 15 h PS, perhaps
559 accounting for the observed earlier sporulation, although the difference diminished at 18-24 h PS
560 (Rajagopalan & Kroos, 2017), as reported here (Fig. 3A). It was concluded that DevI may transiently
561 and weakly inhibit translation of *mrpC* transcripts during the period leading up to commitment,
562 delaying sporulation (Rajagopalan & Kroos, 2017). As noted above, DevI positively autoregulates,
563 causing a small rise in the *dev* transcript level by 30 h PS (Fig. 4A, 7, and 8B). Although the mechanism
564 of this feedback loop is unknown, one possibility is that DevI inhibits negative autoregulation by
565 DevTRS (Fig. 9).
566 In previous studies, mutations in *devT*, *devR*, or *devS* relieved negative autoregulation, resulting in
567 ~10-fold higher *dev* transcript accumulation at 24 h PS (Rajagopalan & Kroos, 2017, Rajagopalan et al.,
568 2015). In this study, a *devS* mutant likewise accumulated ~10-fold more *dev* transcript than WT at 24-

569 30 h PS, and the difference was ~20-fold at 18 and 21 h PS (Fig. 4A), suggesting that negative
570 autoregulation mediated by DevS has a stronger effect leading up to the commitment period than
571 during commitment. Strong negative autoregulation may promote commitment to sporulation by
572 lowering the level of DevI, which would raise the MrpC level by relieving inhibition of translation of
573 *mrpC* transcripts (Rajagopalan & Kroos, 2017). Our data suggest that negative autoregulation by
574 DevTRS weakens during the commitment period, perhaps accounting for the observed small rise in the
575 *dev* transcript level (Fig. 4A, 7, and 8B). If the elevated *dev* transcript level is accompanied by a small
576 increase in the level of DevI, then DevI may inhibit translation of *mrpC* transcripts, causing the MrpC
577 level to decrease slightly by 30 h PS in WT (Fig. 3A). DevI is predicted to be a 40-residue polypeptide
578 (Rajagopalan et al., 2015) and currently no method has been devised to measure the DevI level. This is
579 a worthwhile goal of future research, as is understanding how cells overcome DevI-mediated inhibition
580 of sporulation (depicted in Fig. 9 as inhibition of cellular shape change).
581 In addition to regulating the timing of commitment to spore formation, Dev proteins appear to play
582 a role in maturation of spores. Mutations in *dev* genes strongly impair expression of the *exo* operon
583 (Licking *et al.*, 2000, Rajagopalan & Kroos, 2017), which encodes proteins that help form the
584 polysaccharide spore coat necessary to maintain cellular shape change and form mature spores (Muller
585 *et al.*, 2012, Ueki & Inouye, 2005).
586
587 ***The role of MrpC***
588 Our results add to a growing list of observations that indicate MrpC functions differently during *M.*
589 *xanthus* development than originally proposed. We found that MrpC negatively autoregulates
590 accumulation of *mrpC* mRNA about twofold at 18 and 24 h PS (Fig. S8A), and it does so at 18 h PS

591 without significantly altering transcript stability (Fig. S9). This contradicts an earlier study that
592 concluded MrpC positively autoregulates, based on finding that expression of an *mrpC-lacZ* fusion was
593 abolished in an *mrpC* mutant (Sun & Shi, 2001b). Recently, and in agreement with our result, it was
594 reported that MrpC is a negative autoregulator that competes with MrpB for binding to the *mrpC*
595 promoter region (McLaughlin et al., 2018). MrpB, likely when phosphorylated, binds to two sites
596 upstream of the *mrpC* promoter and activates transcription. MrpC binds to multiple sites upstream of
597 the *mrpC* promoter (Nariya & Inouye, 2006, McLaughlin et al., 2018), including two that overlap the
598 MrpB binding sites (McLaughlin et al., 2018). Purified MrpC competes with the MrpB DNA-binding
599 domain for binding to the overlapping sites, supporting a model in which MrpC negatively
600 autoregulates by directly competing with phosphorylated MrpB for binding to overlapping sites
601 (McLaughlin et al., 2018) (Fig. 9).
602 The role of MrpC in cellular lysis during development appears to be less prominent than originally
603 proposed. MrpC was reported to function as an antitoxin by binding to and inhibiting activity of the
604 MazF toxin protein, an mRNA interferase shown to be important for developmental programmed cell
605 death (Nariya & Inouye, 2008). However, the effect of a null mutation in *mazF* on developmental lysis
606 depends on the presence of a *pilQ1* mutation (Boynton *et al.*, 2013, Lee et al., 2012). In *pilQ*$^{+}$
607 backgrounds such as our WT strain DK1622, MazF is dispensable for lysis. Here, we found only a slight
608 delay of the *mrpC* mutant relative to WT in terms of the declining number of sonication-sensitive cells
609 at 18-48 h PS (Fig. S11A), comparable to other mutants (*csgA*, *fruA*, *devS*, *csgA* P_{van}-*fruA*, *csgA* P_{van}-*fruA*
610 *D59E*) that were unable to form spores (Fig. S1 and S15; Table S1). Under our conditions, MrpC
611 appears to play no special role in modulating the cell number during development.

612 Both the synthesis and the degradation of MrpC are regulated. Synthesis is regulated by
613 phosphorylated MrpB and MrpC acting positively and negatively, respectively, at the level of
614 transcription initiation as described above (McLaughlin et al., 2018) (Fig. 9). Degradation is regulated
615 by the complex Esp signal transduction system (Cho & Zusman, 1999, Higgs *et al.*, 2008, Schramm et
616 al., 2012), which presumably senses a signal and controls the activity of an unidentified protease
617 involved in MrpC turnover, thus ensuring that development proceeds at the appropriate pace (Fig. 9).
618 Interestingly, preliminary results suggest that the Esp system does not govern the proteolysis of MrpC
619 observed when nutrients are added at 18 h PS (Rajagopalan & Kroos, 2014) (Y. Hoang, R. Rajagopalan,
620 and L. Kroos; unpublished data). This implies that another system senses nutrients and degrades MrpC
621 to halt development (Fig. 9).
622
623 ***Combinatorial control by MrpC and FruA***
624 Nutrient-regulated proteolysis of MrpC provides a checkpoint for starvation during the period leading
625 up to and including commitment to sporulation (Rajagopalan & Kroos, 2014) (Fig. 9). If activation of
626 FruA by C-signaling acts as a checkpoint for mound formation as we propose (Fig. 9), then
627 combinatorial control by MrpC and activated FruA could ensure that only starving cells in mounds
628 express genes that commit them to spore formation.
629 MrpC and FruA bind cooperatively to the promoter regions of five C-signal-dependent genes or
630 operons (*dev*, *fmgA*, *fmgBC*, *fmgD*, *fmgE*) (Lee et al., 2011, Mittal & Kroos, 2009a, Mittal & Kroos,
631 2009b, Son et al., 2011, Campbell et al., 2015). In each case, cooperative binding to a site located just
632 upstream of the promoter appears to activate transcription. Hence, MrpC and FruA form a type 1
633 coherent feed-forward loop with AND logic (Mangan & Alon, 2003). This type of loop is abundant in

634 GRNs and can serve as a sign-sensitive delay element (Mangan & Alon, 2003, Mangan *et al.*, 2003).
635 The sign sensitivity refers to a difference in the network response to stimuli in the "OFF to ON"
636 direction versus the "ON to OFF" direction. What this means for the feed-forward loop created by
637 MrpC, FruA, and their target genes is that target gene expression is delayed as MrpC accumulates,
638 awaiting FruA activated by C-signaling (i.e., the "OFF to ON" direction) (Fig. 9). As cells move into
639 mounds and engage in short-range C-signaling, activated FruA would bind cooperatively with MrpC,
640 stimulating transcription of target genes that eventually commit cells to spore formation (depicted in
641 Fig. 9 as cellular shape change). However, if nutrients reappear prior to commitment, MrpC is
642 degraded and transcription of target genes rapidly ceases, halting commitment to sporulation (i.e., the
643 "ON to OFF" direction). The number of target genes may be large since MrpC binds to the promoter
644 regions of hundreds of developmental genes based on ChIP-seq analysis, and in 13 of 15 cases
645 cooperative binding of MrpC and FruA was observed (Robinson et al., 2014).
646 In addition to the feed-forward loop involving cooperative binding of MrpC and FruA to a site
647 located just upstream of the promoter, the promoter regions of some genes have more complex
648 architectures that confer greater dependence on C-signaling for transcriptional activation. For
649 example, in the *fmgD* promoter region, binding of MrpC to an additional site that overlaps the
650 promoter and the FruA binding site appears to repress transcription, and it has been proposed that a
651 high level of active FruA produced by C-signaling is necessary to outcompete MrpC for binding and
652 result in transcriptional activation (Lee et al., 2011) (Fig. S19A). However, the *fmgD* transcript level in
653 WT did not increase significantly from 18 to 30 h PS (Fig. S5 and S18), suggesting that active FruA is not
654 the limiting factor for transcription during this period. In the *fmgE* promoter region, a distal upstream
655 site with higher affinity for cooperative binding of MrpC and FruA appears to act negatively by

656 competing for binding with the lower affinity site just upstream of the promoter (Son et al., 2011) (Fig.
657 S19B). The *fmgE* transcript level in WT did increase significantly from 18 to 30 h (Fig. S5 and S18), but
658 we cannot conclude that active FruA is the limiting factor since LadA also regulates the *fmgE* transcript
659 level during this period (Fig. S5). In addition to *fmgD* and *fmgE*, other genes depend more strongly on
660 C-signaling and are expressed later during development than *dev* (Kroos & Kaiser, 1987). Some of
661 these genes may require a higher level of active FruA than *dev* and *fmgD* in order to be transcribed. In
662 contrast to the *dev* promoter region, which may have a relatively low threshold for active FruA and
663 therefore approach saturation binding of active FruA and MrpC at 18 h PS (Fig. S12), we predict that
664 the promoter regions of genes essential for commitment to sporulation have more complex
665 architectures and a higher threshold for active FruA. According to this model, C-signal-dependent
666 activation of FruA continues after 18 h PS and the rising level of active FruA triggers commitment
667 beginning at 24 h PS. We speculate that genes governing cellular shape change are under
668 combinatorial control of MrpC and FruA (Fig. 9), and have a high threshold for active FruA.
669

670 **Experimental Procedures**

671 ***Bacterial strains, plasmids and primers***

672 The strains, plasmids, and primers used in this study are listed in Table S2. *Escherichia coli* strain DH5α
673 was used for cloning. To construct pSS10, primers FruA-F-NdeI-Gibson and FruA-R-EcoRI-Gibson were
674 used to generate PCR products using chromosomal DNA from *M. xanthus* strain DK1622 as template.
675 The products were combined with NdeI-EcoRI-digested pMR3691 in a Gibson assembly reaction to
676 enzymatically join the overlapping DNA fragments (Gibson *et al.*, 2009). The cloned PCR product was
677 verified by DNA sequencing. To construct pSS9, pSS10 was subjected to site-directed mutagenesis

678 using the Quikchange kit (Stratagene) and primers D59E F and D59E R, and the DNA sequence of the
679 *fruA D59E* gene was verified. *M. xanthus* strains with P_{van}-*fruA* and P_{van}-*fruA D59E* integrated
680 ectopically were constructed by electroporation (Kashefi & Hartzell, 1995) of pSS10 and pSS9,
681 respectively, selection of transformants on CTT agar containing 15 µg/ml of tetracycline (Iniesta *et al.*,
682 2012), and verification by colony PCR using primers pMR3691 MCS G-F and pMR3691 MCS G-R.
683
684 ***Growth and development of* M. xanthus**
685 Strains of *M. xanthus* were grown at 32°C in CTTYE liquid medium (1% Casitone, 0.2% yeast extract, 10
686 mMTris-HCl [pH 8.0], 1 mM KH_2PO_4-K_2HPO_4, 8 mM $MgSO_4$ [final pH 7.6]) with shaking at 350 rpm. CTT
687 agar (CTTYE lacking yeast extract and solidified with 1.5% agar) was used for growth on solid medium
688 and was supplemented with 40 µg/ml of kanamycin sulfate or 15 µg/ml of tetracycline as required.
689 Fruiting body development under submerged culture conditions was performed using MC7 (10 mM
690 morpholinepropanesulfonic acid [MOPS; pH 7.0], 1 mM $CaCl_2$) as the starvation buffer as described
691 previously (Rajagopalan & Kroos, 2014). Briefly, log-phase CTTYE cultures were centrifuged and cells
692 were resuspended in MC7 at a density of approximately 1,000 Klett units. A 100 µl sample (designated
693 T_0) was removed, glutaraldehyde (2% final concentration) was added to fix cells, and the sample was
694 stored at 4°C at least 24 h before total cells were quantified as described below. For each
695 developmental sample, 1.5 ml of the cell suspension plus 10.5 ml of MC7 was added to an 8.5-cm-
696 diameter plastic petri plate. Upon incubation at 32°C, cells adhere to the bottom of the plate and
697 undergo development. At the indicated times developing populations were photographed through a
698 microscope and collected as described below.
699

700 ***Microscopy***

701 Images of fruiting bodies were obtained using a Leica Wild M8 microscope equipped with an Olympus
702 E-620 digital camera. In order to quantify cells in samples collected and dispersed as described below,
703 high resolution images were obtained with an Olympus BX51 microscope using a differential
704 interference contrast filter and a 40× objective lens, and equipped with an Olympus DP30BW digital
705 camera.

706

707 ***Sample collection***

708 At the indicated times the submerged culture supernatant was replaced with 5 ml of fresh MC7
709 starvation buffer with or without inhibitors as required. Developing cells were scraped from the plate
710 bottom using a sterile cell scraper and the entire contents were collected in a 15-ml centrifuge tube.
711 Samples were mixed thoroughly by repeatedly (three times total) vortexing for 15 s followed by
712 pipetting up and down 15 times. For quantification of total cells, 100 μl of the mixture was removed,
713 glutaraldehyde (2% final concentration) was added to fix cells, and the sample was stored at 4°C for at
714 least 24 h before counting as described below. For measurement of sonication-resistant spores, 400 μl
715 of the mixture was removed and stored at -20°C. For immunoblot analysis, 100 μl of the mixture was
716 added to an equal volume of 2× sample buffer (0.125 M Tris-HCl [pH 6.8], 20% glycerol, 4% sodium
717 dodecyl sulfate [SDS], 0.2% bromophenol blue, 0.2 M dithiothreitol), boiled for 5 min, and stored at -
718 20°C. Immediately after collecting the three samples just described, the remaining 4.4 ml of the
719 developing population was mixed with 0.5 ml of RNase stop solution (5% phenol [pH < 7] in ethanol),
720 followed by rapid cooling in liquid nitrogen until almost frozen, centrifugation at 8,700 × *g* for 10 min at
721 4°C, removal of the supernatant, freezing of the cell pellet in liquid nitrogen, and storage at -80°C until

722 RNA extraction. Control experiments with a sample collected at 30 h PS indicated that the majority of
723 spores remain intact after boiling in 2× sample buffer or RNA extraction as described below (data not
724 shown), so the proteins and RNAs analyzed are from developing cells that have not yet formed spores.
725
726 ***Quantification of total cells and sonication-resistant spores***
727 During development a small percentage of the rod-shaped cells transition to ovoid spores that become
728 sonication-resistant. The number of sonication-resistant spores in developmental samples was
729 quantified as described previously (Rajagopalan & Kroos, 2014). Briefly, each 400-μl sample collected
730 as described above was thawed and sonicated using a model 450 sonifier (Branson) at output setting 2
731 for 10-s intervals three times with cooling on ice in between. A 60 μl sample was removed and ovoid
732 spores were counted microscopically using 10 μl in a Neubauer counting chamber. A remaining
733 portion of the sample was used to determine total protein concentration as described below. The total
734 cell number, including rod-shaped cells, ovoid spores, and cells in transition between the two, was
735 determined using the glutaraldehyde-fixed samples collected as described above. Each sample was
736 thawed and mixed by vortexing and pipetting, then 10 or 20 μl was diluted with MC7 to 400 μl,
737 sonicated once for 10 s, and all cells were counted microscopically. The total cell number minus the
738 number of sonication-resistant spores was designated the number of sonication-sensitive cells
739 (consisting primarily of rod-shaped cells) and was expressed as a percentage of the total cell number in
740 the corresponding T_0 sample (consisting only of rod-shaped cells).
741
742 ***RNA extraction and analysis***

743 RNA was extracted using the hot-phenol method and the RNA was digested with DNase I (Roche) as
744 described previously (Higgs et al., 2008). One μg of total RNA was subjected to cDNA synthesis using
745 Superscript III reverse transcriptase (InVitrogen) and random primers (Promega), according to the
746 instructions provided by the manufacturers. Control reactions were not subjected to cDNA synthesis.
747 One μl of cDNA at the appropriate dilution (as determined empirically) and 20 pmol of each primer
748 were subjected to qPCR in a 25 μl reaction using 2× reaction buffer (20 mM Tris-HCl [pH 8.3], 13 mM
749 $MgCl_2$, 100 mM KCl, 400 μM dNTPs, 4% DMSO, 2× SYBR Green I [Molecular Probes], 0.01% Tween 20,
750 0.01% NP40, and 0.01 μg/μl of Taq polymerase) as described previously (Bryant *et al.*, 2008). qPCR
751 was done in quadruplicate for each cDNA using a LightCycler® 480 System (Roche). A standard curve
752 was generated for each set of qPCRs using *M. xanthus* wild-type strain DK1622 genomic DNA and gene
753 expression was quantified using the relative standard curve method (user bulletin 2; Applied
754 Biosystems). 16S rRNA was used as the internal standard for each sample. Relative transcript levels
755 for mutants are the average of three biological replicates after each replicate was normalized to the
756 transcript level observed for one replicate of WT at 18 h PS in the same experiment. Transcript levels
757 for WT at other times PS were likewise normalized to that observed for WT at 18 h PS in the same
758 experiment. For WT at 18 h PS, the transcript levels of at least three biological replicates from
759 different experiments were normalized to their average, which was set as 1.
760
761 ***Immunoblot analysis***
762 A semi-quantitative method of immunoblot analysis was devised to measure the relative levels of
763 MrpC and FruA in many samples collected in different experiments. Equal volumes (10 μl for
764 measurement of MrpC and 15 μl for measurement of FruA) of samples prepared for immunoblot

765 analysis as described above were subjected to SDS-PAGE and immunoblotting as described previously
766 (Rajagopalan & Kroos, 2014, Yoder-Himes & Kroos, 2006). Representative immunoblots for each strain
767 are shown in Figure S20. On each immunoblot, a sample of the wild-type strain DK1622 at 18 h PS
768 served as an internal control for normalization of signal intensities across immunoblots. Signals were
769 detected using a ChemiDoc MP imaging system (Bio-Rad), with exposure times short enough to ensure
770 signals were not saturated, and signal intensities were quantified using Image Lab 5.1 (Bio-Rad)
771 software. After normalization to the internal control, each signal intensity was divided by the total
772 protein concentration of a corresponding sample that had been sonicated for 10-s intervals three times
773 as described above. After removal of a sample for spore quantification, the remaining portion was
774 centrifuged at 10,000 × *g* for 1 min and the total protein concentration of the supernatant was
775 determined using a Bradford (Bradford, 1976) assay kit (Bio-Rad). The resulting values of normalized
776 signal intensity/total protein concentration were further normalized to the average value for all
777 biological replicates of WT at 18 h PS, which was set as 1.
778
779 ***Mathematical modeling***
780 *Activation of dev transcription by FruA and MrpC*
781 FruA and MrpC bind cooperatively to the *dev* promoter region and activate transcription (Campbell et
782 al., 2015). In agreement, no *dev* mRNA was detected in either the *fruA* mutant (Fig. 4A) or the *mrpC*
783 mutant (Fig. 7). We represent the activation of *dev* transcript by FruA and MrpC using a
784 phenomenological Hill's function,

785
$$\Pi_{\mathrm{FM}} = \alpha_{\mathrm{FM}} \left[\frac{\left(\frac{[\mathrm{FruA}][\mathrm{MrpC}]}{\mathrm{K_{FM}}}\right)^{a}}{1 + \left(\frac{[\mathrm{FruA}][\mathrm{MrpC}]}{\mathrm{K_{FM}}}\right)^{a}} \right]$$

786 where α_{FM} denotes the maximal *dev* transcription rate, $\mathrm{K_{FM}}$ is the half-saturation constant, and a

787 denotes the cooperativity of binding. We model the binding cooperativity using a single Hill exponent

788 for the product of the FruA and MrpC concentrations since one FruA and one MrpC bind cooperatively

789 to the proximal site upstream of the *dev* promoter, based on mobility shift assays (Campbell et al., 2015).

790 Note that this expression will give $\Pi_{\mathrm{FM}} = 0$ when $[\mathrm{FruA}] = 0$ or $[\mathrm{MrpC}] = 0$ (i.e., we have neglected

791 any basal transcription rate as we did not detect *dev* mRNA in the *fruA* or *mrpC* mutant. The expression

792 in brackets can be thought as the promoter occupancy probability (P in the equation below), a

793 dimensional parameter telling what fraction of the promoters will be occupied by the transcription

794 factors for a given value of $\mathrm{K_{FM}}$.

795 $$P = \frac{\left(\frac{[\mathrm{FruA}][\mathrm{MrpC}]}{\mathrm{K_{FM}}}\right)^{a}}{1 + \left(\frac{[\mathrm{FruA}][\mathrm{MrpC}]}{\mathrm{K_{FM}}}\right)^{a}}$$

796

797 Note that the sensitivity of this expression to changes in the concentrations of FruA and MrpC are

798 maximal when $P \sim 0$ and minimal near saturation when $P \sim 1$. In Figure 5 we assess how different

799 hypotheses about the role of C-signaling in *dev* regulation play out at different levels of $\mathrm{K_{FM}}$. To facilitate

800 the biological interpretation of the findings, we plot these as a function of *dev* promoter saturation.

801

802 *Feedback regulation by Dev proteins*

803 The *dev* mRNA level is further regulated by Dev proteins DevI and DevS. Our finding that the *dev*

804 transcript level is lower in the *devI* mutant than in WT (Fig. 4A) indicates that DevI is a positive regulator

805 of *dev* mRNA accumulation. In contrast, the *dev* transcript level in the *devS* mutant is significantly higher

806 than in WT (Fig. 4A), indicating that DevS is a negative regulator of *dev* mRNA accumulation. Since the

807 exact mechanisms of regulation by DevI and DevS are unclear, we assume for simplicity that these
808 proteins regulate the *dev* transcript level through independent mechanisms. We model these regulation
809 functions as follows:

810 $$\Pi_{\mathrm{I}} = \left(1 + \alpha_{\mathrm{I}} \frac{\left(\frac{[\mathrm{DevI}]}{\mathrm{K_I}}\right)^b}{1 + \left(\frac{[\mathrm{DevI}]}{\mathrm{K_I}}\right)^b}\right), \qquad \Pi_{\mathrm{S}} = \left(\frac{1}{1 + \left(\frac{[\mathrm{DevS}]}{\mathrm{K_S}}\right)^c}\right)$$

811 Here, α_{I} is a dimensionless parameter characterizing the feedback strength (i.e., the fold-increase in
812 transcription of the *dev* operon due to DevI), $\mathrm{K_I}$ is the half-saturation constant, and *b* denotes effective
813 cooperativity (i.e., Hill coefficient) of DevI binding. Likewise, $\mathrm{K_S}$ is the half-saturation constant and *c*
814 denotes the effective cooperativity of DevS binding. Note that these functions are normalized so that
815 $\Pi_{\mathrm{I}} = 1$ for the *devI* mutant and $\Pi_{\mathrm{S}} = 1$ for the *devS* mutant (i.e., when $[\mathrm{DevI}] = 0$ or $[\mathrm{DevS}] = 0$).

816 We assume that regulation by the Dev proteins is independent of that by FruA and MrpC, and the
817 effects will be multiplicative:

818 $$[\mathrm{mRNA}_{dev}] = \frac{\alpha_{\mathrm{FM}}}{\delta_{dev}} \underbrace{\left(\frac{\left(\frac{[\mathrm{FruA}][\mathrm{MrpC}]}{\mathrm{K_{FM}}}\right)^a}{1 + \left(\frac{[\mathrm{FruA}][\mathrm{MrpC}]}{\mathrm{K_{FM}}}\right)^a}\right)}_{\Pi_{\mathrm{FM}}} \underbrace{\left(1 + \alpha_{\mathrm{I}} \frac{\left(\frac{[\mathrm{DevI}]}{\mathrm{K_I}}\right)^b}{1 + \left(\frac{[\mathrm{DevI}]}{\mathrm{K_I}}\right)^b}\right)}_{\Pi_{\mathrm{I}}} \underbrace{\left(\frac{1}{1 + \left(\frac{[\mathrm{DevS}]}{\mathrm{K_S}}\right)^c}\right)}_{\Pi_{\mathrm{S}}}$$

819 where, $\mathrm{K_{FM}}$, $\mathrm{K_I}$, and $\mathrm{K_S}$ are the saturation constants for regulation by [FruA][MrpC], [DevI], and [DevS],
820 respectively.

821

822 *Numerical procedure to estimate unknown regulation parameters*

823 To explain the difference in the *dev* mRNA level in the *csgA* mutant as compared with WT, in terms of
824 perturbation of potential regulatory mechanisms, we use a mathematical approach where we constrain
825 the FruA ratio ($[\mathrm{FruA}]_{\mathrm{WT}}/[\mathrm{FruA}]_{csgA} \cong 2$) and find the regulation parameters that can result in the

observed 22-fold difference in $[\mathrm{mRNA_{dev}}]$. Specifically, we use the expression of *dev* transcript ratio between WT and the *csgA* mutant below:

$$\frac{[\mathrm{mRNA}_{dev}]_{\mathrm{WT}}}{[\mathrm{mRNA}_{dev}]_{csgA}}$$

$$= \frac{\delta_{dev,csgA}}{\delta_{dev,\mathrm{WT}}} \frac{1+\left(\frac{[\mathrm{FruA}]_{csgA}[\mathrm{MrpC}]_{csgA}}{\mathrm{K_{FM}}}\right)^{a}}{1+\left(\frac{[\mathrm{FruA}]_{\mathrm{WT}}[\mathrm{MrpC}]_{\mathrm{WT}}}{\mathrm{K_{FM}}}\right)^{a}} \left(\frac{[\mathrm{FruA}]_{\mathrm{WT}}[\mathrm{MrpC}]_{\mathrm{WT}}}{[\mathrm{FruA}]_{csgA}[\mathrm{MrpC}]_{csgA}}\right)^{a} \left(\frac{\Pi_{\mathrm{I,WT}}\,\Pi_{\mathrm{S,WT}}}{\Pi_{\mathrm{I},csgA}\Pi_{\mathrm{S},csgA}}\right)$$

$$\frac{[\mathrm{mRNA}_{dev}]_{\mathrm{WT}}}{[\mathrm{mRNA}_{dev}]_{csgA}} = \frac{1}{\delta_R}\left(\frac{R^{a}+\left(\frac{P_{\mathrm{WT}}}{1-P_{\mathrm{WT}}}\right)}{1+\left(\frac{P_{\mathrm{WT}}}{1-P_{\mathrm{WT}}}\right)}\right)\left(\frac{\Pi_{\mathrm{I,WT}}\,\Pi_{\mathrm{S,WT}}}{\Pi_{\mathrm{I},csgA}\Pi_{\mathrm{S},csgA}}\right)$$

where,

$$R = \frac{[\mathrm{FruA}]_{\mathrm{WT}}}{[\mathrm{FruA}]_{csgA}}\frac{[\mathrm{MrpC}]_{\mathrm{WT}}}{[\mathrm{MrpC}]_{csgA}}, \delta_R = \frac{\delta_{dev,\mathrm{WT}}}{\delta_{dev,csgA}} \text{ and } P_{\mathrm{WT}} = \frac{\left(\frac{[\mathrm{FruA}]_{\mathrm{WT}}[\mathrm{MrpC}]_{\mathrm{WT}}}{\mathrm{K_{FM}}}\right)^{a}}{1+\left(\frac{[\mathrm{FruA}]_{\mathrm{WT}}[\mathrm{MrpC}]_{\mathrm{WT}}}{\mathrm{K_{FM}}}\right)^{a}}.$$

First, we estimate the contribution from Dev protein regulation terms $(\Pi_{\mathrm{I}}, \Pi_{\mathrm{S}})$ in determining the *dev* transcript level in WT and the *csgA* mutant. Since we did not measure the Dev proteins explicitly in our experiments, we estimate their contribution in regulating *dev* transcription in WT by comparing the changes in transcript level in their absence (i.e., in the *devI* and *devS* mutants). Based on our transcript data for WT, and the *devI* and *devS* mutants (Fig. 4A), we have the following relations between the regulation functions; $[\mathrm{mRNA}_{dev}]_{\mathrm{WT}} = \delta_{dev,\mathrm{WT}}^{-1}\Pi_{\mathrm{FM,WT}}\Pi_{\mathrm{I,WT}}\Pi_{\mathrm{S,WT}} = 2.9$, $\delta_{dev,\mathrm{WT}}^{-1}\Pi_{\mathrm{FM,WT}}\Pi_{\mathrm{S,WT}} = 1$ and $\delta_{dev,\mathrm{WT}}^{-1}\Pi_{\mathrm{FM,WT}}\Pi_{\mathrm{I,WT}} = 32$. Using these relations, we obtain $\Pi_{\mathrm{I,WT}} = 2.9$, $\Pi_{\mathrm{S,WT}} = 0.091$. For the *csgA* mutant, assuming regulation by Dev proteins is absent due to the low *dev* transcript level, we have $\Pi_{\mathrm{I},csgA} \approx 1$ and $\Pi_{\mathrm{S},csgA} \approx 1$. With these estimates, the above expression for *dev* transcript ratio has three unknown parameters $\delta_R, a, P_{\mathrm{WT}}$.

843 Next, we determine the required fold change in degradation rate δ_R for different promoter
844 saturation probability P_{WT} values that explains the observed 22-fold difference in *dev* transcript. To
845 estimate this, we set the cooperativity constant (a) to 2 and take the fold change in FruA from the
846 experiments, while assuming MrpC is unchanged between WT and the *csgA* mutant. The result is
847 plotted in Fig. 5A. Then, we determine the required cooperativity a for different P_{WT} values with the
848 FruA fold change from the experiments and assuming no change in the degradation rate ($\delta_R = 1$). The
849 result is plotted in Fig. 5B. Finally, we compute the fold change in FruA with $\delta_R = 1$ and $a = 2$ for
850 different P_{WT} values. The result is shown in Fig. 5C.
851
852 ***RNA stability***
853 At the indicated time the submerged culture supernatant was replaced with fresh MC7 starvation
854 buffer supplemented with 50 μg/ml of rifampicin to inhibit RNA synthesis. Samples were collected
855 immediately (designated t_0) and 8 and 16 min later for RNA extraction and analysis as described above,
856 except for each biological replicate the transcript levels after 8 and 16 min were normalized to the
857 transcript level at t_0, which was set as 1, and the natural log of the resulting values was plotted versus
858 minutes after rifampicin treatment and the slope of a linear fit of the data was used to compute the
859 mRNA half-life.
860
861 ***Induction of P_{van}-fruA***
862 To induce expression of *fruA* fused to a vanillate-inducible promoter in *M. xanthus*, the CTTYE growth
863 medium was supplemented with 0.5 mM vanillate when the culture reached 50 Klett units. Growth
864 was continued until the culture reached 100 Klett units, then the culture was centrifuged and cells

865 were resuspended at a density of approximately 1,000 Klett units in MC7 supplemented with 0.5 mM
866 vanillate, followed by submerged culture development as described previously (Rajagopalan & Kroos,
867 2014).
868
869 **Acknowledgements**
870 We thank Monique Floer for advice about high-throughput qPCR and for use of the LightCycler® 480
871 System. We thank Montserrat Elias-Arnanz and Penelope Higgs for sharing strains. This work was
872 supported by the National Science Foundation (award MCB-1411272) and by salary support for L.K.
873 from Michigan State University AgBioResearch.
874
875 **Author contributions**
876 Conception or design of the study: LK, OI, SS, PP
877 Acquisition of the data: SS, PP
878 Analysis or interpretation of the data: SS, PP, LK, OI
879 Writing of the manuscript: LK, SS, PP, OI
880

881 **Graphical abstract**

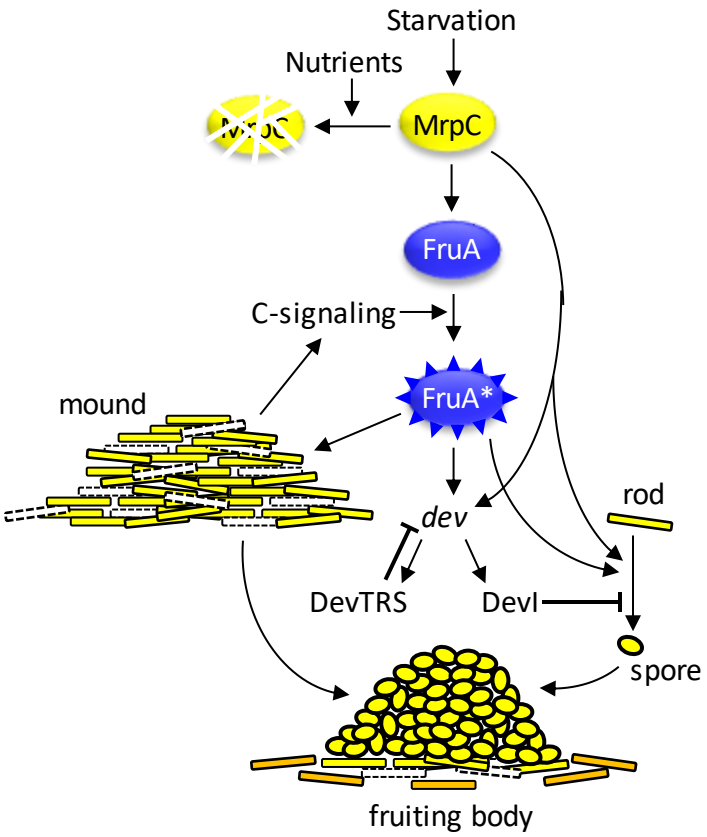

882

883 **Abbreviated summary**

884 Starvation promotes MrpC accumulation, whereas nutrients favor proteolysis. MrpC activates
885 transcription of *fruA*, but FruA protein appears to be activated by short-range C-signaling in a cycle
886 leading to mound formation and lysis of some cells. Activated FruA* and MrpC are proposed to
887 cooperatively stimulate transcription of the *dev* operon and genes that commit starving rod-shaped
888 cells to form spores, while Dev proteins slow commitment, resulting in a spore-filled fruiting body
889 surrounded by peripheral rods.

890

891 **References**

892 Barratt, M. J., C. Lebrilla, H. Y. Shapiro & J. I. Gordon, (2017) The gut microbiota, food science, and human
893 nutrition: a timely marriage. *Cell Host Microbe* **22**: 134-141.

894 Bourret, R. B., (2010) Receiver domain structure and function in response regulator proteins. *Curr. Opin.*
895 *Microbiol.* **13**: 142-149.

896 Boynton, T. O., J. L. McMurry & L. J. Shimkets, (2013) Characterization of *Myxococcus xanthus* MazF and
897 implications for a new point of regulation. *Mol. Microbiol.* **87**: 1267-1276.

898 Boynton, T. O. & L. J. Shimkets, (2015) *Myxococcus* CsgA, *Drosophila* Sniffer and human HSD17B10 are
899 cardiolipin phospholipases. *Genes Dev.* **29**: 1903-1914.

900 Boysen, A., E. Ellehauge, B. Julien & L. Sogaard-Andersen, (2002) The DevT protein stimulates synthesis of FruA,
901 a signal transduction protein required for fruiting body morphogenesis in *Myxococcus xanthus*. *J.*
902 *Bacteriol.* **184**: 1540-1546.

903 Bradford, M., (1976) A rapid and sensitive method for the quantitation of microgram quantities of protein
904 utilizing the principle of protein-dye binding. *Anal. Biochem.* **72**: 248-254.

905 Bretl, D. J. & J. R. Kirby, (2016) Molecular mechanisms of signaling in *Myxococcus xanthus* development. *J. Mol.*
906 *Biol.* **428**: 3805-3830.

907 Bryant, G. O., V. Prabhu, M. Floer, X. Wang, D. Spagna, D. Schreiber & M. Ptashne, (2008) Activator control of
908 nucleosome occupancy in activation and repression of transcription. *PLoS Biol.* **6**: 2928-2939.

909 Bush, M. J., N. Tschowri, S. Schlimpert, K. Flardh & M. J. Buttner, (2015) c-di-GMP signalling and the regulation of
910 developmental transitions in streptomycetes. *Nat. Rev. Microbiol.* **13**: 749-760.

911 Campbell, A., P. Viswanathan, T. Barrett, B. Son, S. Saha & L. Kroos, (2015) Combinatorial regulation of the *dev*
912 operon by MrpC2 and FruA during *Myxococcus xanthus* development. *J. Bacteriol.* **197**: 240-251.

913 Cho, K. & D. R. Zusman, (1999) Sporulation timing in *Myxococcus xanthus* is contolled by the *espAB* locus. *Mol.*
914 *Microbiol.* **34**: 714-725.

915 Davidson, E. H. & M. S. Levine, (2008) Properties of developmental gene regulatory networks. *Proc. Natl. Acad.*
916 *Sci. USA* **105**: 20063-20066.
917 Davlieva, M., Y. Shi, P. G. Leonard, T. A. Johnson, M. R. Zianni, C. A. Arias, J. E. Ladbury & Y. Shamoo, (2015) A
918 variable DNA recognition site organization establishes the LiaR-mediated cell envelope stress response
919 of enterococci to daptomycin. *Nucleic Acids Res.* **43**: 4758-4773.
920 Desai, S. K., R. S. Winardhi, S. Periasamy, M. M. Dykas, Y. Jie & L. J. Kenney, (2016) The horizontally-acquired
921 response regulator SsrB drives a *Salmonella* lifestyle switch by relieving biofilm silencing. *eLife* **5**:
922 e10747.
923 Domian, I. J., K. C. Quon & L. Shapiro, (1997) Cell type-specific phosphorylation and proteolysis of a
924 transcriptional regulator controls the G1-to-S transition in a bacterial cell cycle. *Cell* **90**: 415-424.
925 Drapek, C., E. E. Sparks & P. N. Benfey, (2017) Uncovering gene regulatory networks controlling plant cell
926 differentiation. *Trends Genet.* **33**: 529-539.
927 Ellehauge, E., M. Norregaard-Madsen & L. Sogaard-Andersen, (1998) The FruA signal transduction protein
928 provides a checkpoint for the temporal co-ordination of intercellular signals in *Myxococcus xanthus*
929 development. *Mol. Microbiol.* **30**: 807-817.
930 Frum, T. & A. Ralston, (2015) Cell signaling and transcription factors regulating cell fate during formation of the
931 mouse blastocyst. *Trends Genet.* **31**: 402-410.
932 Galperin, M. Y., (2010) Diversity of structure and function of response regulator output domains. *Curr. Opin.*
933 *Microbiol.* **13**: 150-159.
934 Gibson, D. G., L. Young, R. Y. Chuang, J. C. Venter, C. A. Hutchison, 3rd & H. O. Smith, (2009) Enzymatic assembly
935 of DNA molecules up to several hundred kilobases. *Nat. Methods* **6**: 343-345.
936 Hagen, T. J. & L. J. Shimkets, (1990) Nucleotide sequence and transcriptional products of the *csg* locus of
937 *Myxococcus xanthus*. *J. Bacteriol.* **172**: 15-23.

938 Higgs, P. I., S. Jagadeesan, P. Mann & D. R. Zusman, (2008) EspA, an orphan hybrid histidine protein kinase,
939 regulates the timing of expression of key developmental proteins of *Myxococcus xanthus*. *J. Bacteriol.*
940 **190**: 4416-4426.
941 Iniesta, A. A., F. Garcia-Heras, J. Abellon-Ruiz, A. Gallego-Garcia & M. Elias-Arnanz, (2012) Two systems for
942 conditional gene expression in *Myxococcus xanthus* inducible by isopropyl-β-D-thiogalactopyranoside or
943 vanillate. *J. Bacteriol.* **194**: 5875-5885.
944 Jansson, J. K. & K. S. Hofmockel, (2018) The soil microbiome-from metagenomics to metaphenomics. *Curr. Opin.*
945 *Microbiol.* **43**: 162-168.
946 Kashefi, K. & P. Hartzell, (1995) Genetic supression and phenotypic masking of a *Myxococcus xanthux frzF*$^-$
947 defect. *Molec. Microbiol.* **15**: 483-494.
948 Kim, S. K. & D. Kaiser, (1990a) C-factor: a cell-cell signaling protein required for fruiting body morphogenesis of
949 *M. xanthus*. *Cell* **61**: 19-26.
950 Kim, S. K. & D. Kaiser, (1990b) Cell alignment required in differentiation of *Myxococcus xanthus*. *Science* **249**:
951 926-928.
952 Kim, S. K. & D. Kaiser, (1990c) Cell motility is required for the transmission of C-factor, an intercellular signal that
953 coordinates fruiting body morphogenesis of *Myxococcus xanthus*. *Genes Dev.* **4**: 896-905.
954 Klose, K. E., D. S. Weiss & S. Kustu, (1993) Glutamate at the site of phosphorylation of nitrogen-regulatory
955 protein NTRC mimics aspartyl-phosphate and activates the protein. *J. Mol. Biol.* **232**: 67-78.
956 Kroos, L., (2017) Highly signal-responsive gene regulatory network governing *Myxococcus* development. *Trends*
957 *Genet.* **33**: 3-15.
958 Kroos, L., P. Hartzell, K. Stephens & D. Kaiser, (1988) A link between cell movement and gene expression argues
959 that motility is required for cell-cell signaling during fruiting body development. *Genes Dev.* **2**: 1677-
960 1685.

961 Kroos, L. & D. Kaiser, (1987) Expression of many developmentally regulated genes in *Myxococcus* depends on a
962 sequence of cell interactions. *Genes Dev.* **1**: 840-854.
963 Lan, C. Y. & M. M. Igo, (1998) Differential expression of the OmpF and OmpC porin proteins in *Escherichia coli* K-
964 12 depends upon the level of active OmpR. *J. Bacteriol.* **180**: 171-174.
965 Lee, B., C. Holkenbrink, A. Treuner-Lange & P. I. Higgs, (2012) *Myxococcus xanthus* developmental cell fate
966 production: heterogeneous accumulation of developmental regulatory proteins and reexamination of
967 the role of MazF in developmental lysis. *J. Bacteriol.* **194**: 3058-3068.
968 Lee, J., B. Son, P. Viswanathan, P. Luethy & L. Kroos, (2011) Combinatorial regulation of *fmgD* by MrpC2 and
969 FruA during *Myxococcus xanthus* development. *J. Bacteriol.* **193**: 1681-1689.
970 Licking, E., L. Gorski & D. Kaiser, (2000) A common step for changing cell shape in fruiting body and starvation-
971 independent sporulation of *Myxococcus xanthus*. *J. Bacteriol.* **182**: 3553-3558.
972 Lobedanz, S. & L. Sogaard-Andersen, (2003) Identification of the C-signal, a contact-dependent morphogen
973 coordinating multiple developmental responses in *Myxococcus xanthus*. *Genes Dev.* **17**: 2151-2161.
974 Mangan, S. & U. Alon, (2003) Structure and function of the feed-forward loop network motif. *Proc. Natl. Acad.*
975 *Sci. USA* **100**: 11980-11985.
976 Mangan, S., A. Zaslaver & U. Alon, (2003) The coherent feedforward loop serves as a sign-sensitive delay
977 element in transcription networks. *J. Mol. Biol.* **334**: 197-204.
978 McLaughlin, P. T., V. Bhardwaj, B. E. Feeley & P. I. Higgs, (2018) MrpC, a CRP/Fnr homolog, functions as a
979 negative autoregulator during the *Myxococcus xanthus* multicellular developmental program. *Mol.*
980 *Microbiol.* **109**: 245-261.
981 Mittal, S. & L. Kroos, (2009a) A combination of unusual transcription factors binds cooperatively to control
982 *Myxococcus xanthus* developmental gene expression. *Proc. Natl. Acad. Sci. USA* **106**: 1965-1970.
983 Mittal, S. & L. Kroos, (2009b) Combinatorial regulation by a novel arrangement of FruA and MrpC2 transcription
984 factors during *Myxococcus xanthus* development. *J. Bacteriol.* **191**: 2753-2763.

985 Muller, F. D., C. W. Schink, E. Hoiczyk, E. Cserti & P. I. Higgs, (2012) Spore formation in *Myxococcus xanthus* is
986 tied to cytoskeleton functions and polysaccharide spore coat deposition. *Mol. Microbiol.* **83**: 486-505.
987 Nariya, H. & M. Inouye, (2008) MazF, an mRNA interferase, mediates programmed cell death during
988 multicellular *Myxococcus* development. *Cell* **132**: 55-66.
989 Nariya, H. & S. Inouye, (2005) Identification of a protein Ser/Thr kinase cascade that regulates essential
990 transcriptional activators in *Myxococcus xanthus* development. *Mol. Microbiol.* **58**: 367-379.
991 Nariya, H. & S. Inouye, (2006) A protein Ser/Thr kinase cascade negatively regulates the DNA-binding activity of
992 MrpC, a smaller form of which may be necessary for the *Myxococcus xanthus* development. *Mol.*
993 *Microbiol.* **60**: 1205-1217.
994 Norman, T. M., N. D. Lord, J. Paulsson & R. Losick, (2015) Stochastic switching of cell fate in microbes. *Annu. Rev.*
995 *Microbiol.* **69**: 381-403.
996 O'Connor, K. A. & D. R. Zusman, (1991) Development in *Myxococcus xanthus* involves differentiation into two
997 cell types, peripheral rods and spores. *J. Bacteriol.* **173**: 3318-3333.
998 Ogawa, M., S. Fujitani, X. Mao, S. Inouye & T. Komano, (1996) FruA, a putative transcription factor essential for
999 the development of *Myxococcus xanthus*. *Mol. Microbiol.* **22**: 757-767.
1000 Rajagopalan, R. & L. Kroos, (2014) Nutrient-regulated proteolysis of MrpC halts expression of genes important
1001 for commitment to sporulation during *Myxococcus xanthus* development. *J. Bacteriol.* **196**: 2736-2747.
1002 Rajagopalan, R. & L. Kroos, (2017) The *dev* operon regulates the timing of sporulation during *Myxococcus*
1003 *xanthus* development. *J. Bacteriol.* **199**: e00788-00716.
1004 Rajagopalan, R., S. Wielgoss, G. Lippert, G. J. Velicer & L. Kroos, (2015) *devI* is an evolutionarily young negative
1005 regulator of *Myxococcus xanthus* development. *J Bacteriol* **197**: 1249-1262.
1006 Robinson, M., B. Son & L. Kroos, (2014) Transcription factor MrpC binds to promoter regions of many
1007 developmentally-regulated genes in *Myxococcus xanthus*. *BMC Genomics* **15**: 1123.

1008 Rolbetzki, A., M. Ammon, V. Jakovljevic, A. Konovalova & L. Sogaard-Andersen, (2008) Regulated secretion of a
1009 protease activates intercellular signaling during fruiting body formation in *M. xanthus*. *Dev. Cell* **15**: 627-
1010 634.
1011 Sager, B. & D. Kaiser, (1993) Two cell-density domains within the *Myxococcus xanthus* fruiting body. *Proc. Natl.*
1012 *Acad. Sci. USA* **90**: 3690-3694.
1013 Schramm, A., B. Lee & P. I. Higgs, (2012) Intra- and inter-protein phosphorylation between two hybrid histidine
1014 kinases controls *Myxococcus xanthus* developmental progression. *J. Biol. Chem.* **287**: 25060–25072.
1015 Shimkets, L. J., R. E. Gill & D. Kaiser, (1983) Developmental cell interactions in *Myxococcus xanthus* and the *spoC*
1016 locus. *Proc. Natl. Acad. Sci. USA* **80**: 1406-1410.
1017 Son, B., Y. Liu & L. Kroos, (2011) Combinatorial regulation by MrpC2 and FruA involves three sites in the *fmgE*
1018 promoter region during *Myxococcus xanthus* development. *J. Bacteriol.* **193**: 2756-2766.
1019 Srinivasan, D. & L. Kroos, (2004) Mutational analysis of the *fruA* promoter region demonstrates that C-box and 5-
1020 base-pair elements are important for expression of an essential developmental gene of *Myxococcus*
1021 *xanthus*. *J. Bacteriol.* **186**: 5961-5967.
1022 Stock, A. M., V. L. Robinson & P. N. Goudreau, (2000) Two-component signal transduction. *Annu. Rev. Biochem.*
1023 **69**: 183-215.
1024 Sun, H. & W. Shi, (2001a) Analyses of *mrp* genes during *Myxococcus xanthus* development. *J. Bacteriol.* **183**:
1025 6733-6739.
1026 Sun, H. & W. Shi, (2001b) Genetic studies of *mrp*, a locus essential for cellular aggregation and sporulation of
1027 *Myxococcus xanthus*. *J. Bacteriol.* **183**: 4786-4795.
1028 Thony-Meyer, L. & D. Kaiser, (1993) *devRS*, an autoregulated and essential genetic locus for fruiting body
1029 development in *Myxococcus xanthus*. *J. Bacteriol.* **175**: 7450-7462.

1030 Ueki, T. & S. Inouye, (2003) Identification of an activator protein required for the induction of *fruA*, a gene
1031 essential for fruiting body development in *Myxococcus xanthus*. *Proc. Natl. Acad. Sci. USA* **100**: 8782-
1032 8787.
1033 Ueki, T. & S. Inouye, (2005) Identification of a gene involved in polysaccharide export as a transcription target of
1034 FruA, an essential factor for *Myxococcus xanthus* development. *J. Biol. Chem.* **280**: 32279-32284.
1035 van Gestel, J., H. Vlamakis & R. Kolter, (2015) Division of labor in biofilms: the ecology of cell differentiation.
1036 *Microbiol. Spectr.* **3**: MB-0002-2014.
1037 Viswanathan, P., K. Murphy, B. Julien, A. G. Garza & L. Kroos, (2007a) Regulation of *dev*, an operon that includes
1038 genes essential for *Myxococcus xanthus* development and CRISPR-associated genes and repeats. *J.*
1039 *Bacteriol.* **189**: 3738-3750.
1040 Viswanathan, P., T. Ueki, S. Inouye & L. Kroos, (2007b) Combinatorial regulation of genes essential for
1041 *Myxococcus xanthus* development involves a response regulator and a LysR-type regulator. *Proc. Natl.*
1042 *Acad. Sci. USA* **104**: 7969-7974.
1043 Wang, L., X. Tian, J. Wang, H. Yang, K. Fan, G. Xu, K. Yang & H. Tan, (2009) Autoregulation of antibiotic
1044 biosynthesis by binding of the end product to an atypical response regulator. *Proc Natl Acad Sci U S A*
1045 **106**: 8617-8622.
1046 Yang , Z. & P. Higgs, (2014) Myxobacteria: genomics, cellular and molecular biology. In. Norfolk, UK: Caister
1047 Academic Press, pp.
1048 Yoder-Himes, D. & L. Kroos, (2006) Regulation of the *Myxococcus xanthus* C-signal-dependent Ω4400 promoter
1049 by the essential developmental protein FruA. *J. Bacteriol.* **188**: 5167-5176.

1050

1051

1052

1053 **Figure Legends**

1054 **Fig. 1.** Simplified model of the gene regulatory network governing formation of fruiting bodies.
1055 Starvation increases the level of MrpC early in the process (Sun & Shi, 2001b, Sun & Shi, 2001a, Nariya
1056 & Inouye, 2006). MrpC causes an increase in C-signal (Sun & Shi, 2001a), the product of *csgA* (Hagen &
1057 Shimkets, 1990, Kim & Kaiser, 1990a). MrpC activates transcription of the gene for FruA (Ueki &
1058 Inouye, 2003), and C-signal somehow enhances FruA (Ellehauge et al., 1998) and/or MrpC activity
1059 (Mittal & Kroos, 2009a). MrpC and FruA bind cooperatively to the promoter region of the *dev* operon
1060 and activate transcription (Campbell et al., 2015). The resulting DevTRS proteins negatively
1061 autoregulate (Thony-Meyer & Kaiser, 1993, Viswanathan et al., 2007a, Rajagopalan & Kroos, 2017,
1062 Rajagopalan et al., 2015). DevI delays spore formation within nascent fruiting bodies (Rajagopalan &
1063 Kroos, 2017), but if overproduced, DevI inhibits sporulation (Rajagopalan et al., 2015), which is
1064 promoted by MrpC (Sun & Shi, 2001b) and FruA (Ogawa et al., 1996) activity.

1065

1066 **Fig. 2.** Development of *M. xanthus* strains. Wild-type DK1622 and its indicated mutant derivatives
1067 were subjected to starvation under submerged culture conditions and images were obtained at the
1068 indicated number of hours poststarvation (PS). DK1622 formed mounds by 18 h PS (an arrow points to
1069 one). The *csgA* and *fruA* mutants failed to form mounds, the *devI* mutant was similar to DK1622, and
1070 the *devS* mutant formed mounds later, by 24 h PS, but the mounds failed to darken at later times. Bar,
1071 100 μm. Similar results were observed in at least three biological replicates.

1072

1073 **Fig. 3.** Levels of MrpC and FruA during *M. xanthus* development. Wild-type DK1622 and its indicated
1074 mutant derivatives were subjected to starvation under submerged culture conditions and samples

1075 were collected at the indicated number of hours poststarvation (PS) for measurement of MrpC (A) and
1076 FruA (B) by immunoblot. Graphs show the data points and average of at least three biological
1077 replicates, relative to wild-type DK1622 at 18 h PS, and error bars show one standard deviation.
1078 Asterisks indicate a significant difference ($p < 0.05$ in Student's two-tailed *t*-tests) from wild type at the
1079 corresponding time PS.
1080
1081 **Fig. 4.** Transcript levels during *M. xanthus* development. Wild-type DK1622 and its indicated mutant
1082 derivatives were subjected to starvation under submerged culture conditions and samples were
1083 collected at the indicated number of hours poststarvation (PS) for measurement of *dev* (A), *mrpC* (B),
1084 and *fruA* (C) transcript levels by RT-qPCR. Graphs show the data points and average of at least three
1085 biological replicates, relative to wild-type DK1622 at 18 h PS, and error bars show one standard
1086 deviation. Asterisks indicate a significant difference ($p < 0.05$ in Student's two-tailed *t*-tests) from wild
1087 type at the corresponding time PS.
1088
1089 **Fig. 5.** Mathematical modeling of different hypotheses to explain the low *dev* transcript level in a *csgA*
1090 mutant. Plots showing the required fold change in *dev* transcript degradation rate in the *csgA* mutant
1091 in comparison to wild type (A), cooperativity coefficient for MrpC and FruA binding to the *dev*
1092 promoter region (B), and reduction in FruA activity in the *csgA* mutant in comparison to wild type (C),
1093 to explain the experimental data for different values of promoter saturation.
1094
1095 **Fig. 6.** *dev* transcript stability. Wild-type DK1622 and the *csgA* mutant were subjected to starvation
1096 under submerged culture conditions for 30 h. The overlay was replaced with fresh starvation buffer

1097 containing rifampicin (50 μg/ml) and samples were collected immediately (t_0) and at the times
1098 indicated (t_x) for measurement of the *dev* transcript level by RT-qPCR. Transcript levels at t_x were
1099 normalized to that at t_0 for each of three biological replicates and used to determine the transcript
1100 half-life for each replicate. The average half-life and one standard deviation are reported in the text.
1101 The graph shows the average $\ln(t_x/ t_0)$ and one standard deviation for the three biological replicates of
1102 wild type (black dashed line) and the *csgA* mutant (gray solid line).
1103
1104 **Fig. 7.** *dev* transcript levels. Wild-type DK1622 and its indicated mutant derivative were subjected to
1105 starvation under submerged culture conditions and samples were collected at the indicated number of
1106 hours poststarvation (PS) for measurement of *dev* transcript levels by RT-qPCR. Graphs show the data
1107 points and average of three biological replicates, relative to wild-type DK1622 at 18 h PS, and error
1108 bars show one standard deviation.
1109
1110 **Fig. 8.** FruA protein and *dev* transcript levels. Wild-type DK1622 and its indicated mutant derivatives
1111 were subjected to starvation under submerged culture conditions and samples were collected at the
1112 indicated number of hours poststarvation (PS) for measurement of FruA levels by immunoblot (A) and
1113 *dev* transcript levels by RT-qPCR (B). Graphs show the data points and average of three biological
1114 replicates, relative to wild-type DK1622 at 18 h PS, and error bars show one standard deviation.
1115 Asterisks indicate a significant difference ($p < 0.05$ in Student's two-tailed *t*-tests) from wild type at the
1116 corresponding time PS.
1117

1118 **Fig. 9.** Updated model of the gene regulatory network governing formation of fruiting bodies. Relative
1119 to the simplified model shown in Figure 1 (see legend), this model also includes phosphorylated MrpB
1120 (MrpB-P) which appears to activate transcription of *mrpC*, and negative autoregulation by MrpC which
1121 appears to involve competition with MrpB-P for binding to overlapping sites in the *mrpC* promoter
1122 region; proteolysis of MrpC, which is regulated by the Esp signal transduction system that normally
1123 slows the developmental process and is regulated by nutrient addition that can halt development;
1124 posttranslational activation of FruA to FruA* by C-signaling and promotion of mound formation by
1125 FruA*, thus enhancing short-range C-signaling by bringing cells into proximity; the possibility that DevI
1126 inhibits negative autoregulation by DevTRS; and speculation that the feed-forward loop involving MrpC
1127 and FruA* not only controls transcription of the *dev* operon, but that of genes involved in cellular
1128 shape change as well, committing cells to spore formation and resulting in spore-filled fruiting bodies.
1129 This model deletes activation of MrpC by C-signaling, which was included as a possibility in Figure 1,
1130 but was not supported by our data. See the text for details and references.

Fig. 1

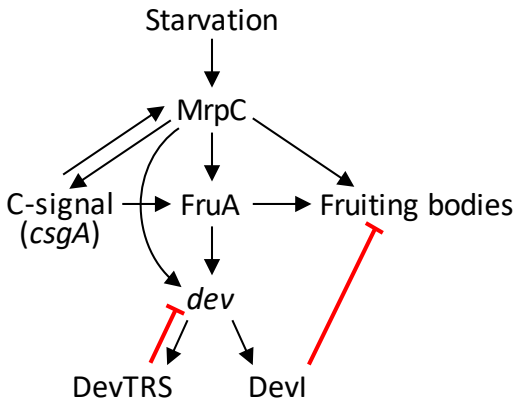
Starvation
MrpC
C-signal
(csgA)
FruA
Fruiting bodies
dev
DevTRS
DevI

Fig. 2

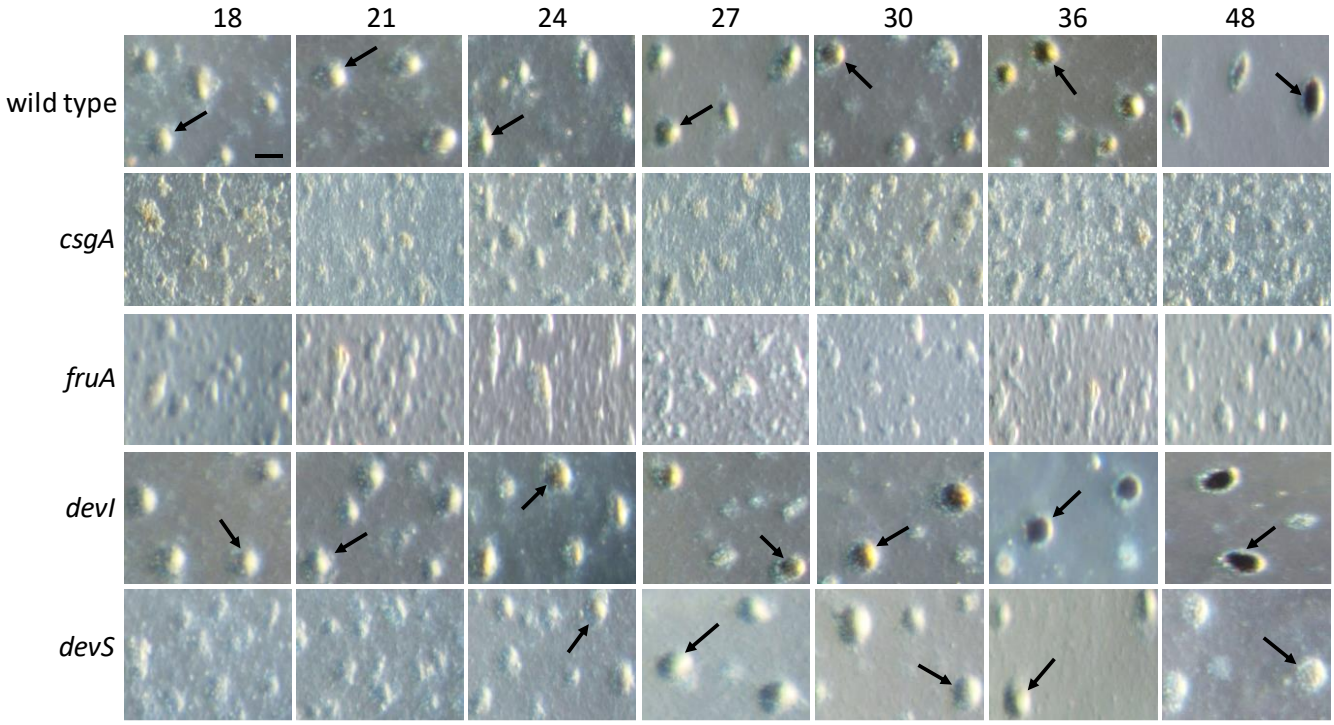

Fig. 3

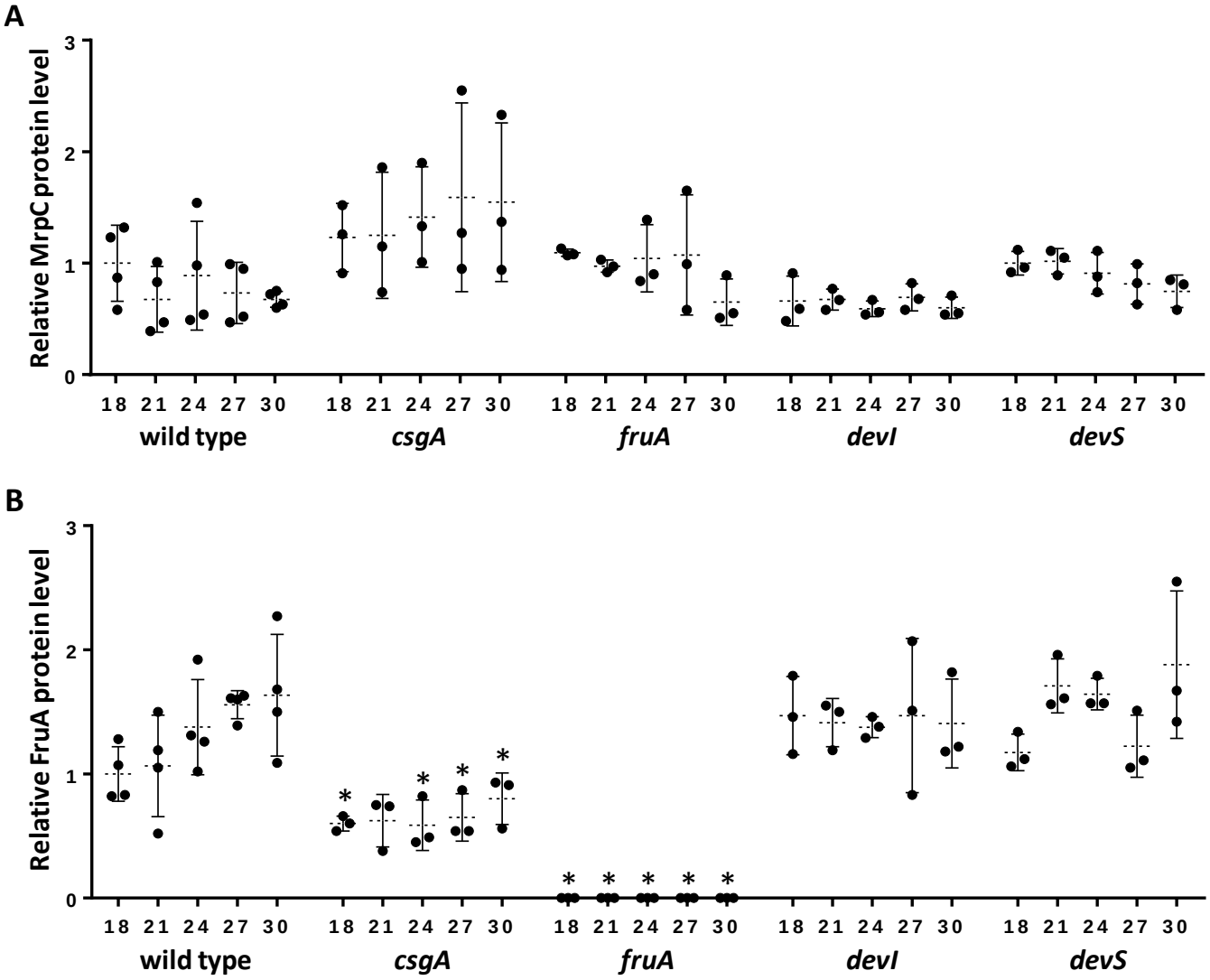
A
Relative MrpC protein level
3
2
1
0
18 21 24 27 30
wild type
csgA
fruA
devI
devS
B
Relative FruA protein level
3
2
1
0
*
wild type
csgA
fruA
devI
devS

Fig. 4

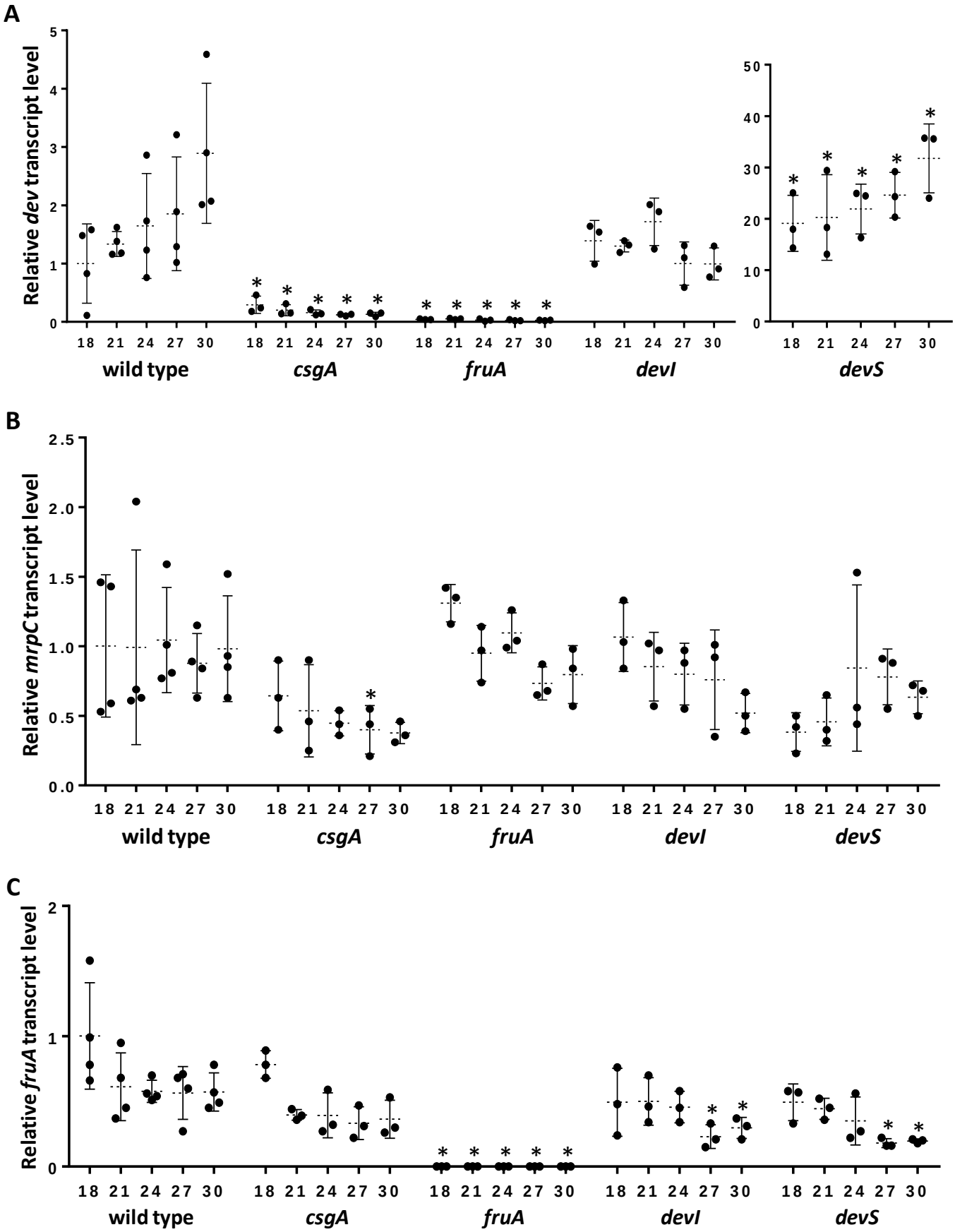
A
Relative dev transcript level
0
1
2
3
4
5
50
40
30
20
10
18 21 24 27 30
wild type
csgA
fruA
devI
devS
B
Relative mrpC transcript level
0.0
0.5
1.0
1.5
2.0
2.5
C
Relative fruA transcript level
0
1
2

Fig. 5

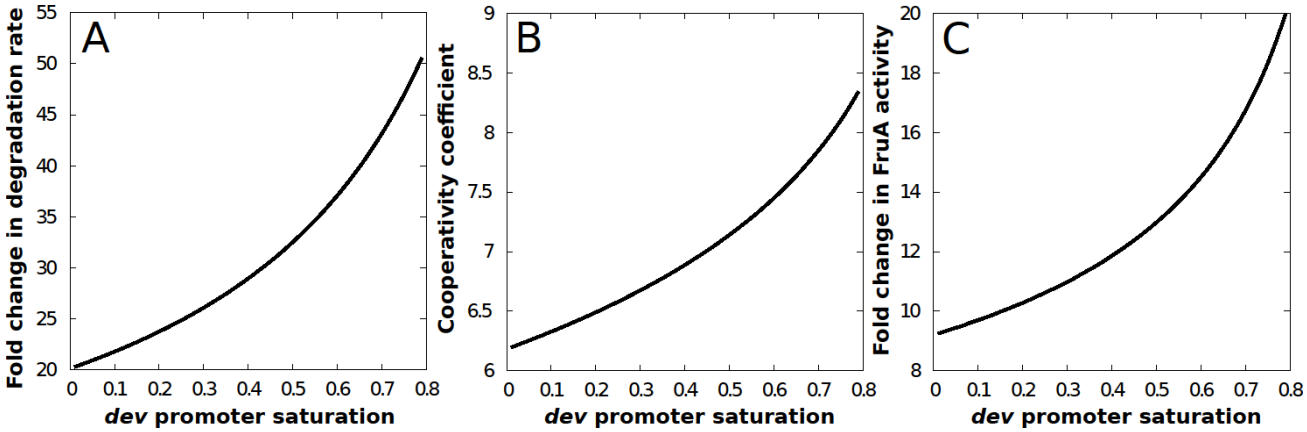
A
Fold change in degradation rate
55
50
45
40
35
30
25
20
0
0.1
0.2
0.3
0.4
0.5
0.6
0.7
0.8
dev promoter saturation
B
Cooperativity coefficient
9
8.5
8
7.5
7
6.5
6
0
0.1
0.2
0.3
0.4
0.5
0.6
0.7
0.8
dev promoter saturation
C
Fold change in FruA activity
20
18
16
14
12
10
8
0
0.1
0.2
0.3
0.4
0.5
0.6
0.7
0.8
dev promoter saturation

Fig. 6

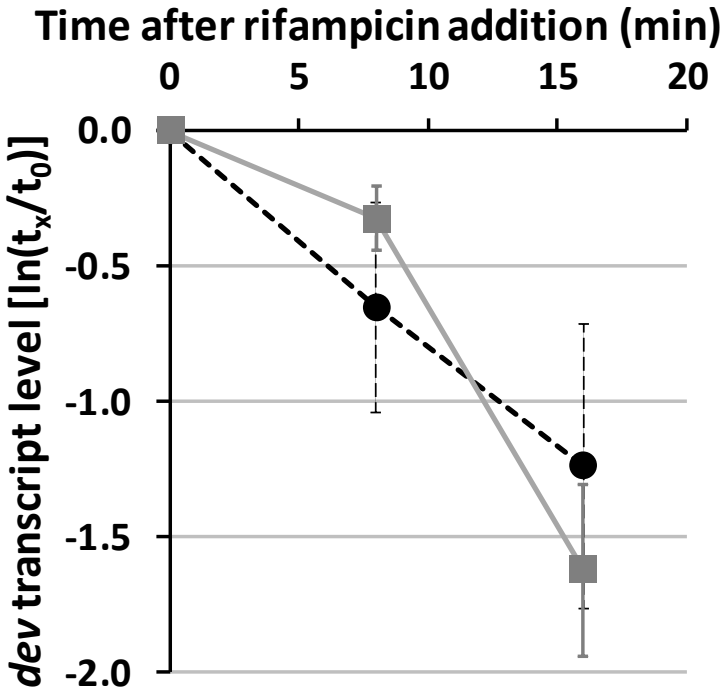
Time after rifampicin addition (min)
0
5
10
15
20
0.0
-0.5
-1.0
-1.5
-2.0
dev transcript level [ln(t_x/t_0)]

Fig. 7

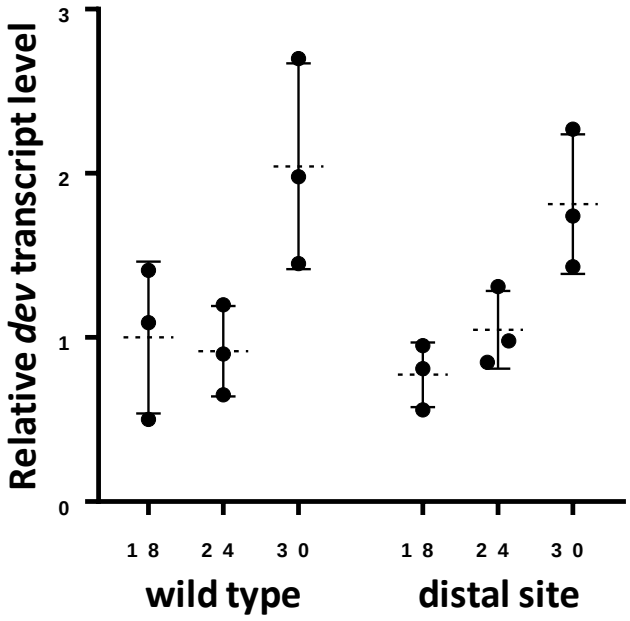
Relative *dev* transcript level
3
2
1
0
1 8
2 4
3 0
1 8
2 4
3 0
wild type
distal site

Fig. 8

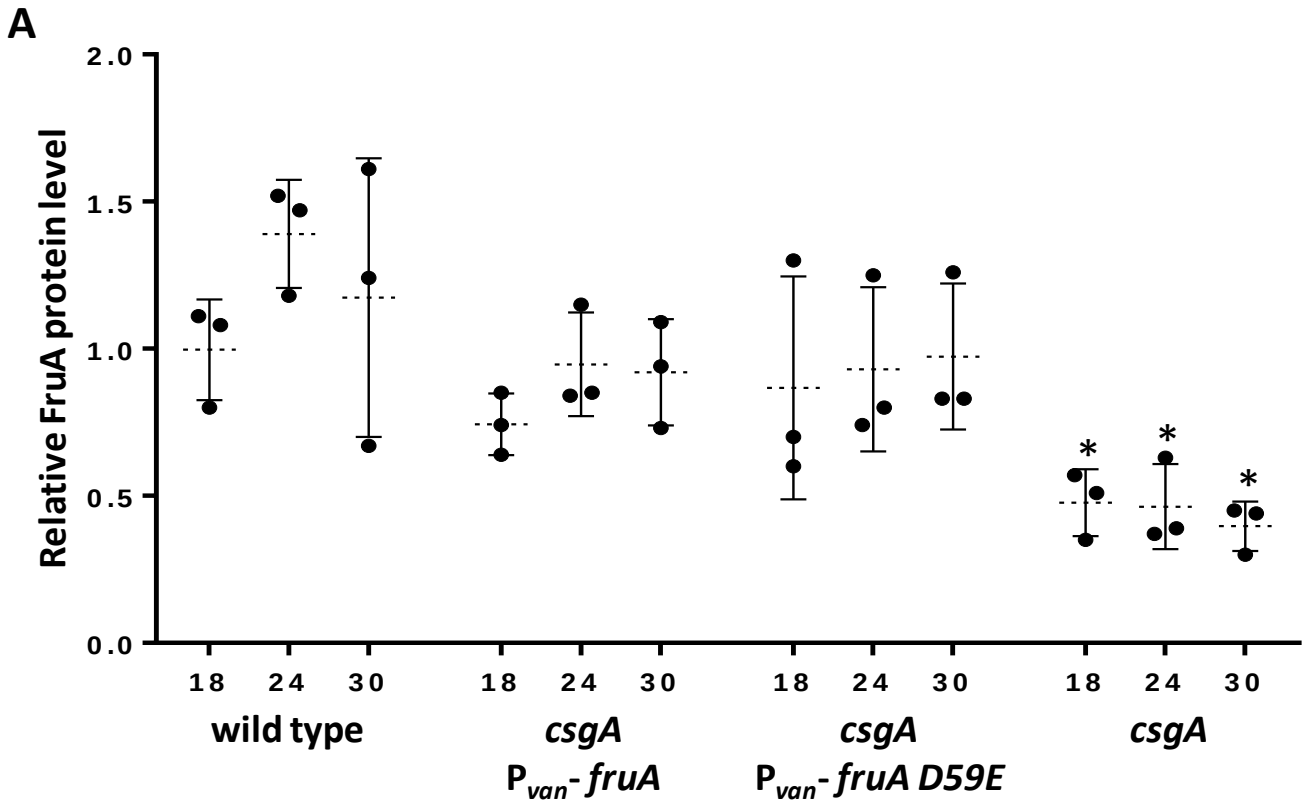
A
Relative FruA protein level
2.0
1.5
1.0
0.5
0.0
18
24
30
wild type
csgA
P$_{van}$- fruA
csgA
P$_{van}$- fruA D59E
csgA
*

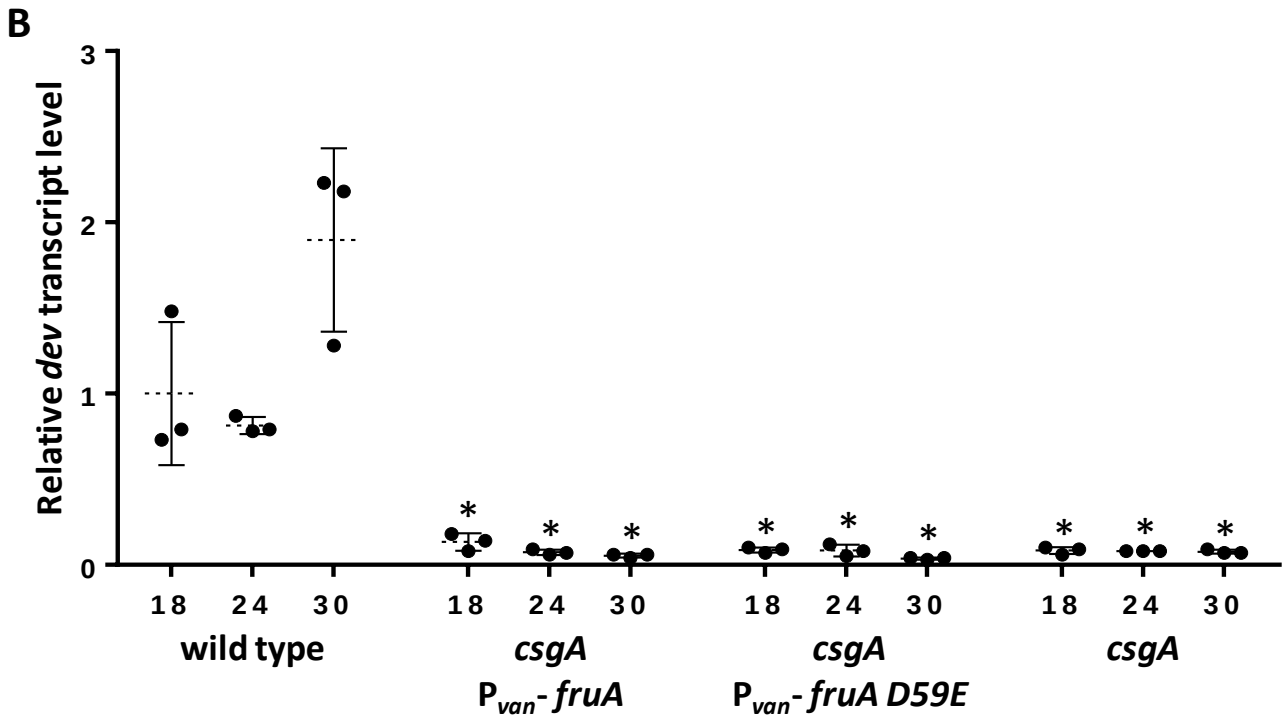
B
Relative dev transcript level
3
2
1
0
18
24
30
wild type
csgA
P$_{van}$- fruA
csgA
P$_{van}$- fruA D59E
csgA
*

Fig. 9

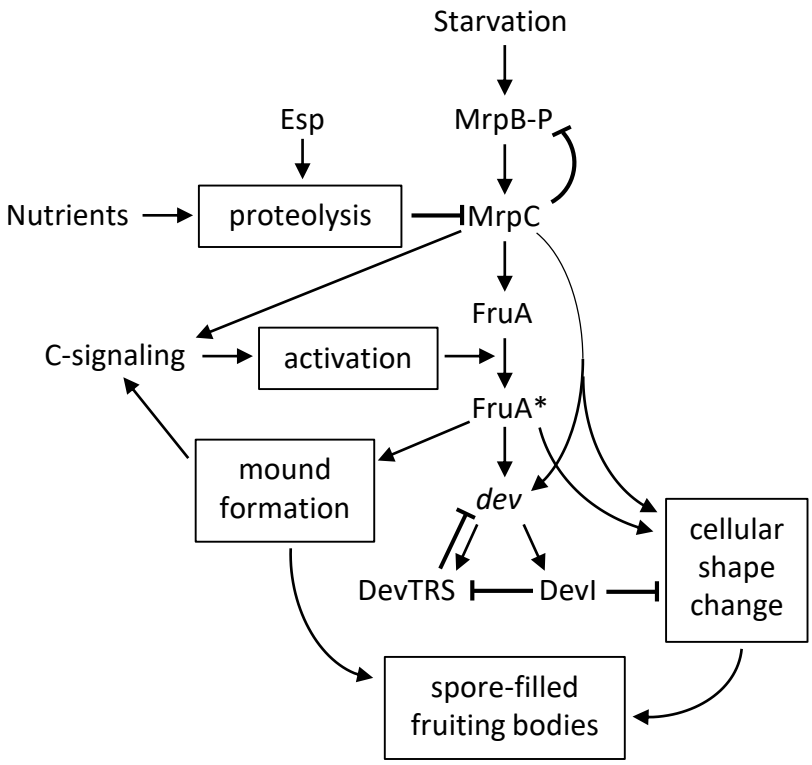
Starvation
Esp
MrpB-P
Nutrients
proteolysis
MrpC
FruA
C-signaling
activation
FruA*
mound formation
dev
cellular shape change
DevTRS
DevI
spore-filled fruiting bodies